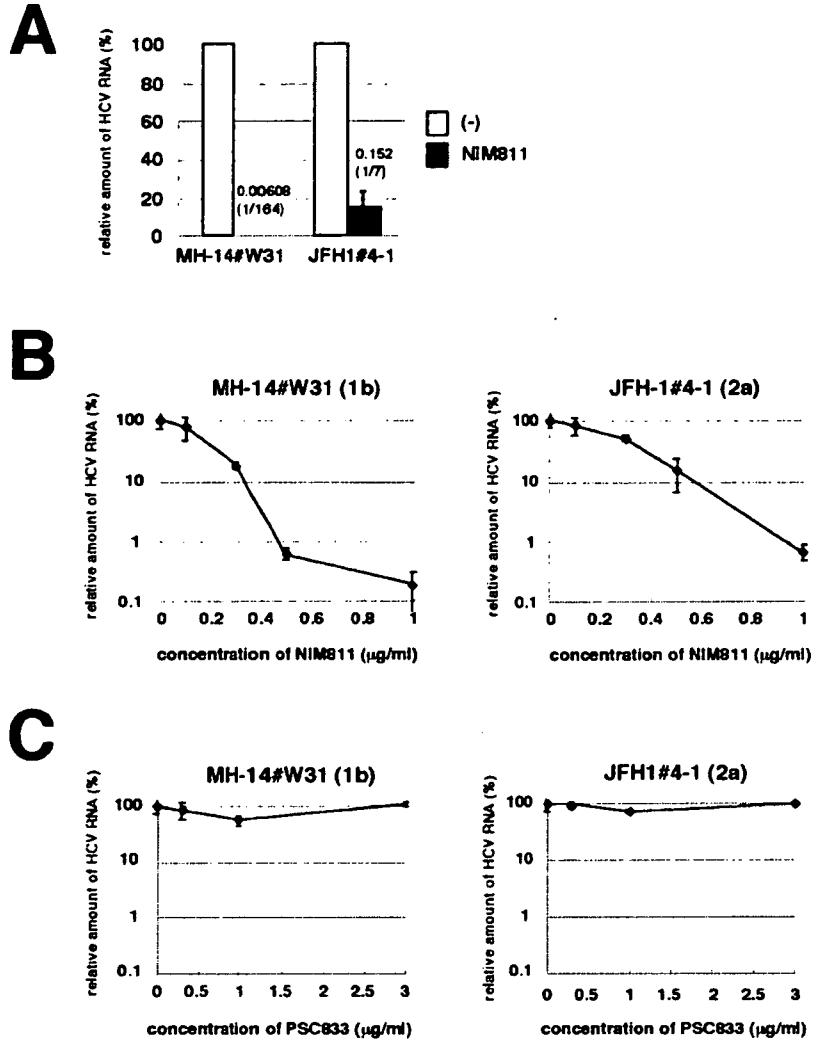

FIG. 4. JFH1 replication was less sensitive to a CsA derivative, NIM811. (A) MH14#W31 (NN/1b/SG) and JFH1#4-1 (JFH1/2a/SG) cells were treated with 0.5-μg/ml NIM811 for 7 days. HCV RNA titers were quantified as described in the legend to Fig. 3A. White bars, no treatment; black bars, 0.5-μg/ml NIM811. (B and C) HCV RNA in replicon cells treated with various concentrations of NIM811 (B) or PSC833 (C) for 7 days was quantified and plotted against the concentration of NIM811 (B) or PSC833 (C) (in micrograms per milliliter) as described in the legend to Fig. 3C.

cellular genome (data not shown). Similarly, we generated other full-genome replicon cells carrying sequences from the Con1 strain at the nonstructural coding region of the replicon RNA (SN1A#2 [Con1/1b/FL]) and SNC#7 (Con1/1b/FL) cells (Fig. 1). The replicon of SN1A#2 (Con1/1b/FL) cells possessed the EMCV IRES upstream of the open reading frame for HCV proteins, while that of SNC#7 (Con1/1b/FL) cells contained the HCV IRES (Fig. 1). SNC#7 (Con1/1b/FL) cells exhibited almost the same response as that of SN1A#2 (Con1/1b/FL) cells to CsA treatment (Fig. 2D). Consistent with a previous report (22), the EMCV IRES was not responsible for the anti-HCV activity of CsA. We compared the sensitivity to CsA of full-genome replicons with that of subgenomic replicons. CsA strongly decreased the production of HCV proteins in both the full-genome replicon, NNC#2 (NN/1b/FL) cells and the subgenomic replicon, MH-14 (NN/1b/SG) cells (Fig. 2C). Real-time RT-PCR analysis also revealed a dramatic reduction of the RNA level of full-genome replicons in NNC#2 (NN/1b/FL), SN1A#2 (Con1/1b/FL), and SNC#7 (Con1/1b/FL) cells (Fig. 2D). The 50% inhibitory concentrations (IC_{50}) of CsA in NNC#2 (NN/1b/FL), SN1A#2 (Con1/1b/FL), and SNC#7 (Con1/1b/FL) cells awere estimated to be 0.13, 0.19, and 0.24 μg/ml, respectively. The 90% inhibitory concentrations (IC_{90}) of CsA in these cells were 0.68, 0.94, and 0.81 μg/ml, respectively. The CsA dose-response curves of full-genome replicons and subgenomic replicons were similar (i.e., compare SN1A#2 or SNC#7 [Con1/1b/FL] versus SN1 [Con1/1b/SG], NNC#2 [NN/1b/FL] versus MH-14, #50-1, or MH14#W31 [NN/1b/SG]) (Fig. 3C). These results demonstrate that CsA suppresses the replication of full-genome replicons and subgenomic replicons to almost the same extent. Since CsA concentrations of up to 3 μg/ml did not affect the

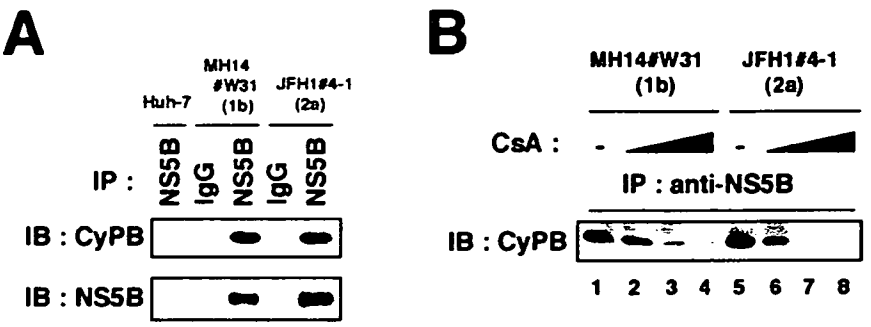

FIG. 5. Interaction of HCV NS5B with CyPB in the JFH1 replicon. (A) Coimmunoprecipitation of endogenous CyPB with NS5B. Lysates from MH14#W31 (NN/1b/SG), JFH1#4-1 (JFH1/2a/SG), and Huh-7 cells as a negative control were used for immunoprecipitation with normal mouse immunoglobulin G (IgG) or anti-NS5B antibody (NS5B), followed by immunoblot analysis with either anti-CyPB (top) or anti-NS5B antibodies (bottom). IP, antibodies used for immunoprecipitation. (B) The interaction of CyPB with NS5B in JFH1 replicon was disrupted by CsA treatment. Coimmunoprecipitation between CyPB and NS5B was analyzed with MH14#W31 (NN/1b/SG) or JFH1#4-1 (JFH1/2a/SG) cells treated without CsA (lanes 1 and 5) or with CsA (0.3 μg/ml in lanes 2 and 6, 1 μg/ml in lanes 3 and 7, and 3 μg/ml in lanes 4 and 8).

proliferation of any replicon cells (Fig. 2E and data not shown), the effect of CsA on replication is not due to the cytotoxic effect. In addition, we observed the reduction of production of infectious viral particles in the presence of 3-μg/ml CsA (data not shown) using the viral production system with full-genome JFH1 RNA (27).

The JFH1 replicon was less sensitive to CsA than were genotype 1b replicons. We compared the sensitivity of HCV replication to CsA in several subgenomic replicon cells. We used MH-14 (NN/1b/SG) and #50-1 (NN/1b/SG) cells carrying subgenomic replicons with HCV NN strain (15, 29), SN1 (Con1/1b/SG) cells carrying the Con1 subgenomic replicon (18), and sO (O/1b/SG) cells bearing the subgenomic O strain (12) as genotype 1b replicon-containing cells. We also employed JFH1#4-1 (JFH1/2a/SG) and JFH1#2-3 (JFH1/2a/SG) cell clones carrying the JFH1 subgenomic replicon (13). Treatment of CsA (1 μg/ml; 7 days) drastically decreased HCV RNA in all the subgenomic replicon cells carrying the HCV genotype 1b strain. HCV RNA levels in SN1 (Con1/1b/SG), MH-14 (NN/1b/SG), sO (O/1b/SG), and #50-1 (NN/1b/SG) cells decreased to 1/134, 1/219, 1/128, and 1/295, respectively (Fig. 3A). Genotype 1b replicon cells appeared highly sensitive to CsA. In contrast, the effect of CsA on HCV RNA levels in replicon cells containing sequences from the JFH1 strain was limited to 1/5 to 1/7 (Fig. 3A). These results of the response to CsA were reproduced in further additional cell clones.

The cellular characteristics of Huh-7 cell strains differ among laboratories. To exclude the possibility that differences between Huh-7 cell strains influence the sensitivity to CsA, we established genotype 1b replicon cells based on the identical Huh-7 cell strain, which were used as parental cells of JFH1#4-1 (JFH1/2a/SG) and JFH1#2-3 (JFH1/2a/SG) cells. The response of the corresponding replicon cells, MH14#W31 (NN/1b/SG), to CsA was almost the same as that of SN1 (Con1/1b/SG), MH-14 (NN/1b/SG), sO (O/1b/SG), and #50-1 (NN/1b/SG) cells (Fig. 3C). Thus, the difference in sensitivity of JFH1 and genotype 1b strains to CsA can be attributed to the characteristic differences of the HCV strains, not to the parental Huh-7 cell strain. In addition, the reduction of NS3 protein in JFH1#4-1 (JFH1/2a/SG) cells following treatment with CsA was less prominent than that in MH14#W31 (NN/1b/SG) cells (Fig. 3B).

We examined the dose-response curve of HCV RNA against the concentration of CsA (Fig. 3C). The effect of CsA in genotype 1b replicons plateaued at around 1 μg/ml, while in the dose-response curve in JFH1 replicon, the inhibition was not yet saturated (Fig. 3C). As concentrations of CsA up to 3 μg/ml did not affect the proliferation rate of any replicon cells (Fig. 3D and data not shown), the effect of CsA on replication was not due to the cytotoxic effect. The IC_{50} of CsA in MH-14 (NN/1b/SG), #50-1 (NN/1b/SG), MH14#W31 (NN/1b/SG), SN1 (Con1/1b/SG), sO (O/1b/SG), JFH1#4-1 (JFH1/2a/SG), and JFH1#2-3 (JFH1/2a/SG) cells were estimated to be 0.15, 0.18, 0.16, 0.20, 0.25, 0.67, and 0.43 μg/ml, respectively. The IC_{90} was 0.86, 0.82, 0.76, 0.88, 0.92, 2.77, and 2.39 μg/ml, respectively. A similar dose-response curve in the JFH1 replicon was obtained by a transient replication assay with the luciferase reporter driven from a JFH1 replicon construct (data not shown) (14).

JFH1 replicon was less sensitive to a CsA derivative, NIM811. Analysis of several CsA derivatives has revealed that the anti-HCV effect of CsA on the genotype 1b replicon is mediated by the inhibition of CyP (31). We examined the sensitivity of JFH1 replicon to CsA derivatives. CsA is known to have three major cellular targets: CyP, calcineurin (CN)/NF-AT, and P glycoprotein (P-gp) (28, 31). A CsA derivative, NIM811, inhibits CyP and P-gp but not CN/NF-AT, while another derivative, PSC833, inhibits P-gp but neither CyP nor CN/NF-AT (31). The decrease of HCV RNA in MH14#W31 (NN/1b/SG) cells with NIM811 treatment (0.5 μg/ml; 7 days) was more than an order of magnitude greater than that in JFH1#4-1 (JFH1/2a/SG) cells (Fig. 4A). The slope of the dose-response curve of NIM811 treatment of the JFH1 replicon was gentler than that of genotype 1b (Fig. 4B). The IC_{50} of NIM811 in MH14W#31 (NN/1b/SG) and JFH1#4-1 (JFH1/2a/SG) cells were 0.17 and 0.30 μg/ml, respectively. The IC_{90} were 0.46 and 0.93 μg/ml, respectively. In contrast, PSC833, which does not inhibit CyP, did not alter HCV RNA level in either genotype 1b or the JFH1 replicon (Fig. 4C). Thus, a CyP

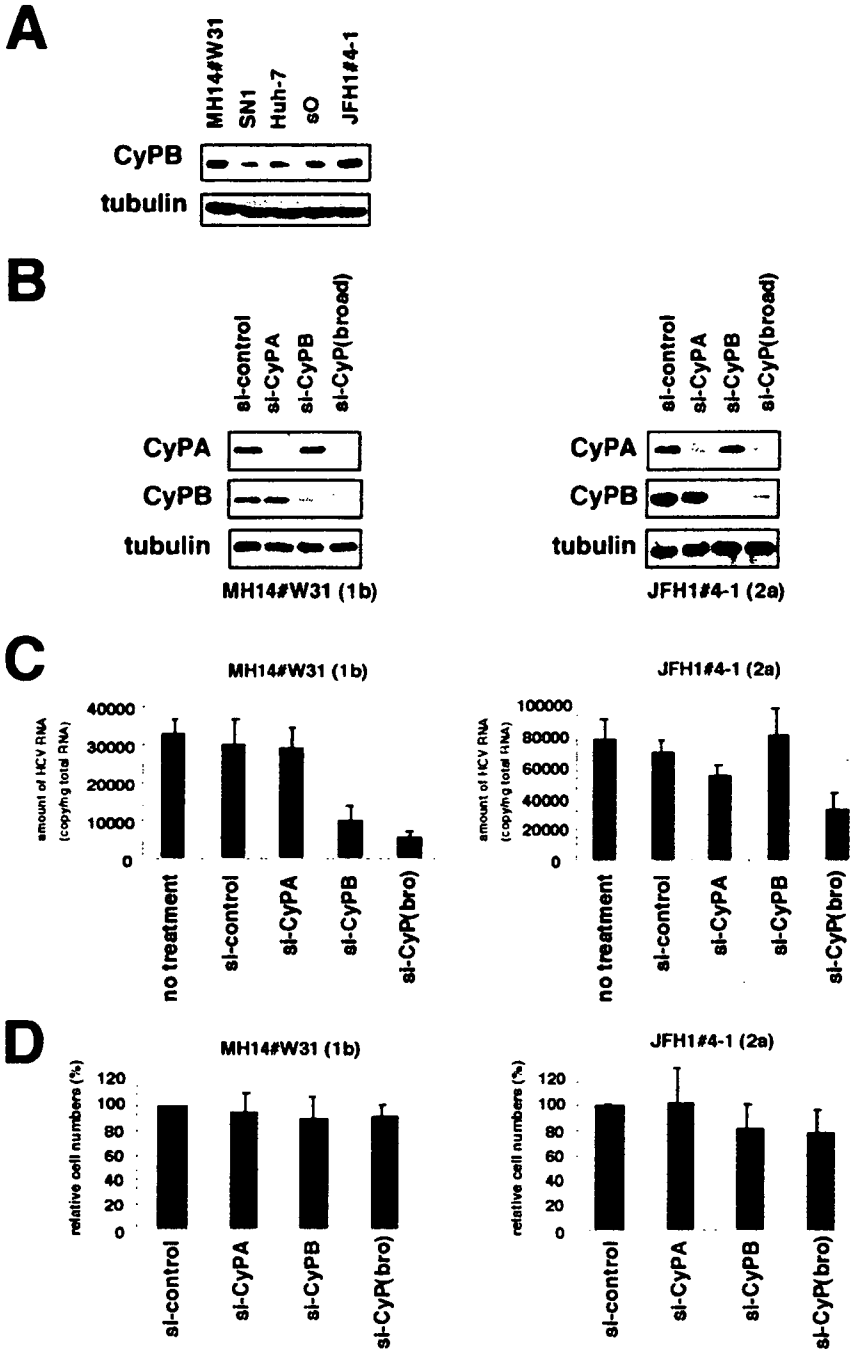

FIG. 6. CyPB in HCV replication of genotype 1b and JFH1. (A) Expression level of endogenous CyPB protein (top) and tubulin as an internal control (bottom) in MH14#W31 (NN/1b/SG), SN1 (Con1/1b/SG), sO (O/1b/SG), JFH1#4-1 (JFH1/2a/SG), and Huh-7 cells. (B) Knockdown of endogenous CyP proteins. MH14#W31 (NN/1b/SG) and JFH1#4-1 (JFH1/2a/SG) cells were transfected with siRNA specific for CyPA (si-CyPA), CyPB (si-CyP), a broad range of CyP subtypes [si-CyP(broad)], or a randomized siRNA (si-control). At 72 h posttransfection, CyPA (top), CyPB (middle) and tubulin as an internal control (bottom) were detected in total cell lysates of MH14#W31 (NN/1b/SG) (left) and JFH1#4-1 (JFH1/2a/SG) (right) cells by immunoblot analysis. (C) Depletion of CyPB did not affect HCV replication of JFH1 replicon. At 5 days posttransfection, HCV RNA titers in MH14#W31 (NN/1b/SG) (left) and JFH1#4-1 (JFH1/2a/SG) (right) cells were quantified by real-time RT-PCR analysis. no treatment, treatment with only the transfection reagent in the absence of siRNA. (D) Effect of siRNA on cell proliferation. Cell numbers of MH14W#31 (NN/1b/SG) and JFH1#4-1 (JFH1/2a/SG) cells treated with siRNA for 5 days were counted. Relative cell numbers were indicated.

inhibitor was less effective at suppressing the replication of the JFH1 replicon than genotype 1b replicons.

Interactions between CyPB and JFH1 NS5B. Previously, we have shown that CyPB interacts with NS5B to promote HCV genome replication and that CsA inhibits this binding in a genotype 1b replicon (31). Here, we examined the association between CyPB and NS5B in a JFH1 replicon. Immunoprecipitation analysis revealed an interaction of CyPB with NS5B in JFH1#4-1 (JFH1/2a/SG) cells (Fig. 5A). This interaction was dissociated following the treatment of CsA, as observed with the genotype 1b replicon (Fig. 5B).

Role of CyPB in replication of the JFH1 replicon. Although we observed some differences of expression levels of endogenous CyPB among the replicon cells in the immunoblot analysis (Fig. 6A), there was no particular correlation between endogenous CyPB expression levels and replication sensitivity to CsA among cells. CyPB reportedly regulates HCV genome replication of the genotype 1b replicon (31). We then explored the requirement of CyPB for the replication of JFH1 replicon with RNA interference. Transfecting siRNAs designed to recognize several CyP subtypes [si-CyP(broad)] (Fig. 6B) reduced HCV RNA to <1/5 in MH14#W31 (NN/1b/SG) cells (Fig. 6C). Specific knockdown of CyPB but not CyPA (Fig. 6B) decreased HCV RNA in MH14#W31 (NN/1b/SG) cells, consistent with a previous report (Fig. 6C) (31). In contrast, HCV RNA in JFH1#4-1 (JFH1/2a/SG) cells was not altered following the suppression of either endogenous CyPA or CyPB (Fig. 6B and C). We observed a weak decrease of HCV RNA levels (around one-half) with si-CyP(broad) (Fig. 6C). These data suggests the possibility that the replication of the JFH1 replicon is independent of CyPB, in contrast to the genotype 1b replicon. In the previous study, it was reported that the doubling time, saturation density, and response to cell confluence of the replicon cells carrying JFH1 were different from those in cells carrying a genotype 1b replicon, suggesting the possibility that the coupling relationship between the replication and cell growth was different between genotype 1b and the JFH1 replicon (21). The introduction of either si-CyPB or si-CyP(broad), however, had little effect on cell growth in MH14#W31 (NN/1b/SG) or JFH1#4-1 (JFH1/2a/SG) cells (Fig. 6D). And we did not observe cells being confluent in the experiment period. The above results suggest that the different response to si-CyPB in the two lines is independent of the conditions of cell growth.

The role of CyPB in the RNA binding activity of JFH1 NS5B. CyPB regulates HCV genome replication of a genotype 1b replicon by promoting the RNA binding activity of NS5B (31). We examined the effect of CyPB on the RNA binding activity of NS5B in JFH1. NS5B in the replication complex was isolated from cells by treatment with digitonin-proteinase K, as described previously (31). This fraction was incubated with poly(U) RNA-Sepharose or protein G-Sepharose as a negative control for the detection of RNA binding NS5B in the replication complex. RNA-bound NS5B in this fraction from MH14#W31 (NN/1b/SG) cells was decreased drastically following treatment with CsA (Fig. 7A, lanes 5 and 6). However, the reduction of RNA binding of NS5B in the replication complex of JFH1#4-1 (JFH1/2a/SG) cells was not as prominent (Fig. 7A, lanes 11 and 12). We confirmed this result by an in vitro RNA binding assay, in which in vitro-synthesized NS5B was incubated with poly(U) RNA-Sepharose, together with

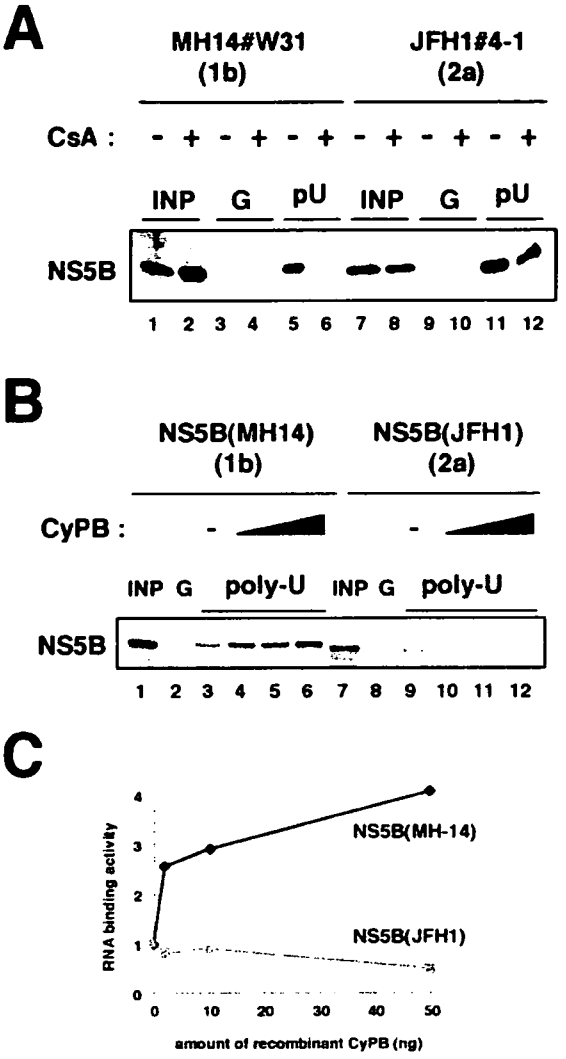

FIG. 7. RNA binding capacity of JFH1 NS5B was independent of CyPB. (A) An RNA-protein binding precipitation assay was performed using MH14#W31 (NN/1b/SG) cells (lanes 1 to 6) and JFH1#4-1 (JFH1/2a/SG) cells (lanes 7 to 12) as described in Materials and Methods. MH14#W31 (NN/1b/SG) and JFH1#4-1 (JFH1/2a/SG) cells preincubated without (lanes 1, 3, 5, 7, 9, and 11) or with (lanes 2, 4, 6, 8, 10, and 12) CsA were treated with digitonin, followed by digestion with proteinase K to isolate the replication complex. This fraction was then incubated with poly(U) RNA-Sepharose (lanes 5, 6, 11, and 12) or protein G-Sepharose as a negative control (lanes 3, 4, 9, and 10). Precipitates were detected by immunoblot analysis with anti-NS5B antibody. INP, one-sixth of the amount of cell lysate used in the precipitation assay; G and pU, samples with protein G-Sepharose and poly(U)-Sepharose, respectively. (B) An in vitro RNA binding assay was performed as described in Materials and Methods. In vitro-synthesized NS5B of MH-14 (lanes 1 to 6) or JFH1 (lanes 7 to 12) with the rabbit reticulocyte lysate in the presence of [^{35}S]methionine was incubated with protein G-Sepharose (lanes 2 and 8) or poly(U)-Sepharose in the absence (lanes 3 and 9) or presence of various amounts of purified recombinant GST-CyPB (2 ng in panels 4 and 10, 10 ng in panels 5 and 11, and 50 ng in panels 6 and 12). The resultant precipitates were fractionated by sodium dodecyl sulfate-polyacrylamide gel electrophoresis, followed by the detection of radiolabeled protein. (C) The density of the bands of NS5B in the RNA binding fraction was quantified and plotted against the amount of the recombinant GST-CyPB (in nanograms). Solid line, NS5B of MH-14; faint line, NS5B of JFH1.

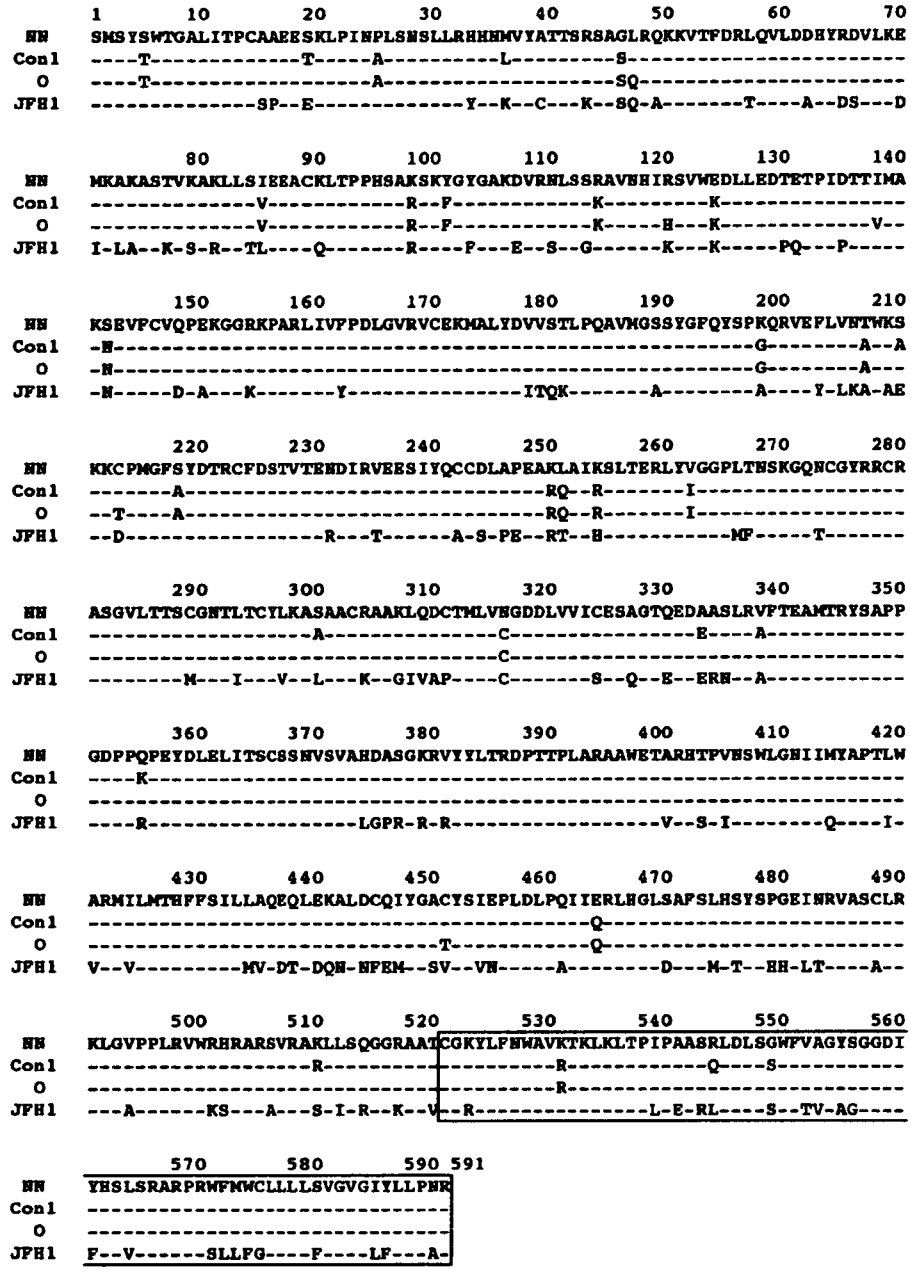

FIG. 8. Amino acid sequence alignment of NS5B encoded by HCV strains NN, Con1, O, and JFH1. The numbers above the sequence indicate the amino acid numbers. Conserved residues are shown by dashes. The region spanning 521 to 591 aa, which is involved in the interaction with CyPB, is boxed.

recombinant GST-CyPB. The addition of recombinant GST-CyPB increased the binding of genotype 1b NS5B to poly(U) RNA (Fig. 7B and C). However, this augmentation of RNA binding was not observed with NS5B from the JFH1 strain (Fig. 7B and C). From the above results, it is suggested that the RNA binding of JFH1 NS5B is free from regulation by CyPB.

DISCUSSION

Until now, we and another group have utilized subgenomic replicons carrying genotype 1b NN and HCV-N strains to demonstrate that CsA suppresses HCV genome replication (22, 29). This study reveals that CsA is effective on full-genome replicons to almost the same extent. In addition, other available genotype 1b replicons carrying the Con1 and O strains also have a high sensitivity to CsA, consistent with our proposal that HCV genotype 1b is highly sensitive to CsA. However, a fulminant-type genotype 2a replicon, JFH1, was less responsive to CsA, although a high dose of CsA suppressed the replication of this strain.

CyPB interacts with genotype 1b NS5B to stimulate its RNA

binding activity. In contrast, CyPB binds JFH1 NS5B but does not regulate the function of JFH1 NS5B. This is consistent with a previous speculation that genotype 1b and JFH1 replicons utilize the same cellular factors in distinct manners (21). The NS5B sequence of NN strain has 95.0, 95.9, and 70.4% homology to that of Con1, O, and JFH1, respectively (Fig. 8). The region spanning amino acids (aa) 521 to 591 of NS5B, which is involved in the interaction with CyPB (31), is highly conserved among genotype 1b strains NN, Con1, and O while that of JFH1 has 21 substituted residues in this region. The proline at 540 aa, which is important for CyPB binding (31), is conserved but the adjacent residues such as isoleucine at 539 aa and alanine at 541 aa are replaced by leucine and glutamic acid, respectively, in JFH1. Through molecular interactions, CyPB seems to make the conformation of NS5B of genotype 1b strains but not JFH1 suitable for RNA binding (31). The diverse regulation system of NS5B by CyPB among strains may be due to differences in either the sequence or the entire conformation of NS5B. Further study is important for elucidating the regulation mechanism of RNA binding activity of NS5B by CyPB.

Thus, replication in JFH1 replicon is independent of CyPB. Interestingly, human immunodeficiency virus type 1 (HIV-1) strains also have a diversity of CyP dependence on viral proliferation (3, 33). CyPA plays an important role in the life cycle of HIV-1. The interaction of the HIV-1 capsid protein with CyPA that resides within the target cells of infection is critical for HIV-1 replication (7, 24). In peripheral blood mononuclear cells or Jurkat T cells, CsA suppresses the proliferation of HIV-1 group main (M) strain (3). However, certain strains of group outlier (O), such as MVP5180 and MVP9435, are resistant to CsA (3, 33), suggesting the different dependency of the replication on CyPA. Authors have suggested that MVP5180 and MVP9435 clones adapt to replicate independently of CyPA and that this adaptation provides a significant replication advantage for the virus in vivo (3). In vesicular stomatitis virus (VSV) strains, a role for CyPA in virus replication also has been reported (2). CyPA is required for the infection of the VSV-NJ strain but not the VSV-IND strain. These authors proposed that during evolutionary divergence from the ancestral lineages that initially were dependent on CyPA for replication, VSV-IND may have adapted to reduce its dependency on CyPA (2). In the case of HCV, a fulminant type genotype 2a replicon (JFH1) replicates independently of CyPB. It has previously been reported that JFH1 has a much higher competency of replication in the cells than other strains (13). The adaptation to independence from CyPB may contribute to the high capacity of replication of JFH1.

Although the JFH1 replicon is less sensitive to CsA, high concentrations of CsA still suppress replication of the JFH1 replicon. Moreover, the introduction of the siRNA designed to recognize several CyP subtypes [si-CyP(broad)] moderately diminishes HCV RNA in the JFH1 replicon. We suspect that a CyP family member other than CyPB is involved in HCV genome replication. Further analysis is needed on the role of other CyP subtypes.

As there a replicon system for a fulminant-type genotype 1b replicon or chronic-type genotype 2a replicon does not yet exist, we cannot conclude whether chronic-type genotype 2a replicons or fulminant-type replicons are less sensitive to CsA or not. However, there is a clinical report describing cotreatment of patients with chronic hepatitis C with IFN and CsA that resulted in a higher sustained virological rate than with treatment of IFN alone (11). In this report, increase in the sustained virological rate was prominent with patients carrying genotype 1 HCV (51.7% versus 21.9%), while it was relatively weak in patients carrying genotype 2 HCV (66.7% versus 58.3%) (11). Thus, genotype may affect the sensitivity of HCV replication to CsA. However, we cannot exclude the possibility that the diminished sensitivity to CsA is a characteristic only of the fulminant-type genotype 2a strain.

Our results suggest that sensitivity to CsA and replication dependency to CyPB is different among HCV strains. This finding is an important insight into the diversity of the mechanism of HCV genome replication and its sensitivity to antiviral agents.

ACKNOWLEDGMENTS

We thank H. Takahashi and M. Hosaka for preparing replicon cells and generating plasmids. We are grateful to A. Takamizawa at Osaka University, I. Fukuya at Osaka University, and M. Kohara at Tokyo Metropolitan Institute of Medical Science for antibodies and R. Bartenschlager at Heiderberg University for the I377/NS3-3′ sequence. We also appreciate Novartis (Basel, Switzerland) for providing the CsA derivatives NIM811 and PSC833.

This work was supported by grants-in-aid for cancer research and for the second-term comprehensive 10-year strategy for cancer control from the Ministry of Health, Labor, and Welfare; grants-in-aid for scientific research from the Ministry of Education, Culture, Sports, Science and Technology; and grants-in-aid from the Research for the Future from the Japanese Society for the Promotion of Science, the Program for Promotion of Fundamental Studies in Health Science of the Organization for Pharmaceutical Safety and Research of Japan, and Research on Health Sciences focusing on Drug Innovation from the Japan Health Sciences Foundation.

REFERENCES

1. **Bartenschlager, R., and V. Lohmann.** 2001. Novel cell culture systems for the hepatitis C virus. Antiviral Res. 52:1–17.
2. **Bose, S., M. Mathur, P. Bates, N. Joshi, and A. K. Banerjee.** 2003. Requirement for cyclophilin A for the replication of vesicular stomatitis virus New Jersey serotype. J. Gen. Virol. 84:1687–1699.
3. **Braaten, D., E. K. Franke, and J. Luban.** 1996. Cyclophilin A is required for the replication of group M human immunodeficiency virus type 1 (HIV-1) and simian immunodeficiency virus $SIV_{CPZ}GAB$ but not group O HIV-1 or other primate immunodeficiency viruses. J. Virol. 70:4220–4227.
4. **Bukh, J., R. H. Purcell, and R. H. Miller.** 1994. Sequence analysis of the core gene of 14 hepatitis C virus genotypes. Proc. Natl. Acad. Sci. USA 91:8239–8243.
5. **Frese, M., V. Schwarzle, K. Barth, N. Krieger, V. Lohmann, S. Mihm, O. Haller, and R. Bartenschlager.** 2002. Interferon-gamma inhibits replication of subgenomic and genomic hepatitis C virus RNAs. Hepatology 35:694–703.
6. **Grakoui, A., C. Wychowski, C. Lin, S. M. Feinstone, and C. M. Rice.** 1993. Expression and identification of hepatitis C virus polyprotein cleavage products. J. Virol. 67:1385–1395.
7. **Hatziioannou, T., D. Perez-Caballero, S. Cowan, and P. D. Bieniasz.** 2005. Cyclophilin interactions with incoming human immunodeficiency virus type 1 capsids with opposing effects on infectivity in human cells. J. Virol. 79: 176–183.
8. **Hijikata, M., H. Mizushima, T. Akagi, S. Mori, N. Kakiuchi, N. Kato, T. Tanaka, K. Kimura, and K. Shimotohno.** 1993. Two distinct proteinase activities required for the processing of a putative nonstructural precursor protein of hepatitis C virus. J. Virol. 67:4665–4675.
9. **Hosui, A., K. Ohkawa, H. Ishida, A. Sato, F. Nakanishi, K. Ueda, T. Takehara, A. Kasahara, Y. Sasaki, M. Hori, and N. Hayashi.** 2003. Hepatitis C virus core protein differently regulates the JAK-STAT signaling pathway under interleukin-6 and interferon-gamma stimuli. J. Biol. Chem. 278:28562–28571.
10. **Ikeda, M., M. Yi, K. Li, and S. M. Lemon.** 2002. Selectable subgenomic and genome-length dicistronic RNAs derived from an infectious molecular clone of the HCV-N strain of hepatitis C virus replicate efficiently in cultured Huh7 cells. J. Virol. 76:2997–3006.
11. **Inoue, K., K. Sekiyama, M. Yamada, T. Watanabe, H. Yasuda, and M.**

Yoshiba. 2003. Combined interferon α2b and cyclosporin A in the treatment of chronic hepatitis C: controlled trial. J. Gastroenterol. **38**:567–572.
12. **Kato, N., K. Sugiyama, K. Namba, H. Dansako, T. Nakamura, M. Takami, K. Naka, A. Nozaki, and K. Shimotohno.** 2003. Establishment of a hepatitis C virus subgenomic replicon derived from human hepatocytes infected in vitro. Biochem. Biophys. Res. Commun. **306**:756–766.
13. **Kato, T., T. Date, M. Miyamoto, A. Furusaka, K. Tokushige, M. Mizokami, and T. Wakita.** 2003. Efficient replication of the genotype 2a hepatitis C virus subgenomic replicon. Gastroenterology **125**:1808–1817.
14. **Kato, T., T. Date, M. Miyamoto, M. Sugiyama, Y. Tanaka, E. Orito, T. Ohno, K. Sugihara, I. Hasegawa, K. Fujiwara, K. Ito, A. Ozasa, M. Mizokami, and T. Wakita.** 2005. Detection of anti-hepatitis C virus effects of interferon and ribavirin by a sensitive replicon system. J. Clin. Microbiol. **43**:5679–5684.
15. **Kishine, H., K. Sugiyama, M. Hijikata, N. Kato, H. Takahashi, T. Noshi, Y. Nio, M. Hosaka, Y. Miyanari, and K. Shimotohno.** 2002. Subgenomic replicon derived from a cell line infected with the hepatitis C virus. Biochem. Biophys. Res. Commun. **293**:993–999.
16. **Liang, T. J., and T. Heller.** 2004. Pathogenesis of hepatitis C-associated hepatocellular carcinoma. Gastroenterology **127**:S62–S71.
17. **Lindenbach, B. D., M. J. Evans, A. J. Syder, B. Wolk, T. L. Tellinghuisen, C. C. Liu, T. Maruyama, R. O. Hynes, D. R. Burton, J. A. McKeating, and C. M. Rice.** 2005. Complete replication of hepatitis C virus in cell culture. Science **309**:623–626.
18. **Lohmann, V., F. Korner, J. Koch, U. Herian, L. Theilmann, and R. Bartenschlager.** 1999. Replication of subgenomic hepatitis C virus RNAs in a hepatoma cell line. Science **285**:110–113.
19. **Manns, M. P., J. G. McHutchison, S. C. Gordon, V. K. Rustgi, M. Shiffman, R. Reindollar, Z. D. Goodman, K. Koury, M. Ling, and J. K. Albrecht.** 2001. Peginterferon alfa-2b plus ribavirin compared with interferon alfa-2b plus ribavirin for initial treatment of chronic hepatitis C: a randomised trial. Lancet **358**:958–965.
20. **McHutchison, J. G., S. C. Gordon, E. R. Schiff, M. L. Shiffman, W. M. Lee, V. K. Rustgi, Z. D. Goodman, M. H. Ling, S. Cort, J. K. Albrecht, et al.** 1998. Interferon alfa-2b alone or in combination with ribavirin as initial treatment for chronic hepatitis C. N. Engl. J. Med. **339**:1485–1492.
21. **Miyamoto, M., T. Kato, T. Date, M. Mizokami, and T. Wakita.** 2006. Comparison between subgenomic replicons of hepatitis C virus genotypes 2a (JFH-1) and 1b (Con1 NK5.1). Intervirology **49**:37–43.
22. **Nakagawa, M., N. Sakamoto, N. Enomoto, Y. Tanabe, N. Kanazawa, T. Koyama, M. Kurosaki, S. Maekawa, T. Yamashiro, C. H. Chen, Y. Itsui, S. Kakinuma, and M. Watanabe.** 2004. Specific inhibition of hepatitis C virus replication by cyclosporin A. Biochem. Biophys. Res. Commun. **313**:42–47.
23. **Ohno, O., M. Mizokami, R. R. Wu, M. G. Saleh, K. Ohba, E. Orito, M. Mukaide, R. Williams, and J. Y. Lau.** 1997. New hepatitis C virus (HCV) genotyping system that allows for identification of HCV genotypes 1a, 1b, 2a, 2b, 3a, 3b, 4, 5a, and 6a. J. Clin. Microbiol. **35**:201–207.
24. **Sokolskaja, E., D. M. Sayah, and J. Luban.** 2004. Target cell cyclophilin A modulates human immunodeficiency virus type 1 infectivity. J. Virol. **78**: 12800–12808.
25. **Taylor, D. R., S. T. Shi, P. R. Romano, G. N. Barber, and M. M. Lai.** 1999. Inhibition of the interferon-inducible protein kinase PKR by HCV E2 protein. Science **285**:107–110.
26. **Tellinghuisen, T. L., and C. M. Rice.** 2002. Interaction between hepatitis C virus proteins and host cell factors. Curr. Opin. Microbiol. **5**:419–427.
27. **Wakita, T., T. Pietschmann, T. Kato, T. Date, M. Miyamoto, Z. Zhao, K. Murthy, A. Habermann, H. G. Krausslich, M. Mizokami, R. Bartenschlager, and T. J. Liang.** 2005. Production of infectious hepatitis C virus in tissue culture from a cloned viral genome. Nat. Med. **11**:791–796.
28. **Waldmeier, P. C., K. Zimmermann, T. Qian, M. Tintelnot-Blomley, and J. J. Lemasters.** 2003. Cyclophilin D as a drug target. Curr. Med. Chem. **10**:1485–1506.
29. **Watashi, K., M. Hijikata, M. Hosaka, M. Yamaji, and K. Shimotohno.** 2003. Cyclosporin A suppresses replication of hepatitis C virus genome in cultured hepatocytes. Hepatology **38**:1282–1288.
30. **Watashi, K., M. Hijikata, A. Tagawa, T. Doi, H. Marusawa, and K. Shimotohno.** 2003. Modulation of retinoid signaling by a cytoplasmic viral protein via sequestration of Sp110b, a potent transcriptional corepressor of retinoic acid receptor, from the nucleus. Mol. Cell. Biol. **23**:7498–7509.
31. **Watashi, K., N. Ishii, M. Hijikata, D. Inoue, T. Murata, Y. Miyanari, and K. Shimotohno.** 2005. Cyclophilin B is a functional regulator of hepatitis C virus RNA polymerase. Mol. Cell **19**:111–122.
32. **Watashi, K., and K. Shimotohno.** 2003. The roles of hepatitis C virus proteins in modulation of cellular functions: a novel action mechanism of the HCV core protein on gene regulation by nuclear hormone receptors. Cancer Sci. **94**:937–943.
33. **Wiegers, K., and H. G. Krausslich.** 2002. Differential dependence of the infectivity of HIV-1 group O isolates on the cellular protein cyclophilin A. Virology **294**:289–295.
34. **Zhong, J., P. Gastaminza, G. Cheng, S. Kapadia, T. Kato, D. R. Burton, S. F. Wieland, S. L. Uprichard, T. Wakita, and F. V. Chisari.** 2005. Robust hepatitis C virus infection in vitro. Proc. Natl. Acad. Sci. USA **102**:9294–9299.

JOURNAL OF VIROLOGY, Mar. 2006, p. 2832–2841 Vol. 80, No. 6
0022-538X/06/$08.00+0 doi:10.1128/JVI.80.6.2832–2841.2006

Subcellular Localization of Hepatitis C Virus Structural Proteins in a Cell Culture System That Efficiently Replicates the Virus

Yves Rouillé,[1] François Helle,[1] David Delgrange,[1] Philippe Roingeard,[2] Cécile Voisset,[1] Emmanuelle Blanchard,[1] Sandrine Belouzard,[1] Jane McKeating,[3] Arvind H. Patel,[4] Geert Maertens,[5] Takaji Wakita,[6] Czeslaw Wychowski,[1]† and Jean Dubuisson[1]*†

CNRS-UPR2511, Institut de Biologie de Lille–Institut Pasteur de Lille, Lille, France[1]; INSERM-ESPRI3856, François Rabelais University, Tours, France[2]; Institute of Biomedical Research, University of Birmingham, Birmingham, United Kingdom[3]; MRC Virology Unit, Institute of Virology, Glasgow, United Kingdom[4]; Innogenetics, Ghent, Belgium[5]; and Department of Microbiology, Tokyo Metropolitan Institute for Neuroscience, Tokyo, Japan[6]

Received 23 September 2005/Accepted 23 December 2005

Due to the recent development of a cell culture model, hepatitis C virus (HCV) can be efficiently propagated in cell culture. This allowed us to reinvestigate the subcellular localization of HCV structural proteins in the context of an infectious cycle. In agreement with previous reports, confocal immunofluorescence analysis of the subcellular localization of HCV structural proteins indicated that, in infected cells, the glycoprotein heterodimer is retained in the endoplasmic reticulum. However, in contrast to other studies, the glycoprotein heterodimer did not accumulate in other intracellular compartments or at the plasma membrane. As previously reported, an association between the capsid protein and lipid droplets was also observed. In addition, a fraction of labeling was consistent with the capsid protein being localized in a membranous compartment that is associated with the lipid droplets. However, in contrast to previous reports, the capsid protein was not found in the nucleus or in association with mitochondria or other well-defined intracellular compartments. Surprisingly, no colocalization was observed between the glycoprotein heterodimer and the capsid protein in infected cells. Electron microscopy analyses allowed us to identify a membrane alteration similar to the previously reported "membranous web." However, no virus-like particles were found in this type of structure. In addition, dense elements compatible with the size and shape of a viral particle were seldom observed in infected cells. In conclusion, the cell culture system for HCV allowed us for the first time to characterize the subcellular localization of HCV structural proteins in the context an infectious cycle.

Hepatitis C virus (HCV) is a small enveloped virus that belongs to the *Hepacivirus* genus in the *Flaviviridae* family (27). Its genome encodes a single polyprotein precursor of ~3,010 amino acid residues, which is synthesized on endoplasmic reticulum (ER)-associated ribosomes. The polyprotein is cleaved co- and posttranslationally by cellular and viral proteases to yield at least 10 mature products. HCV genome encodes three structural proteins: a capsid protein (C) and two envelope glycoproteins (E1 and E2). These proteins are released from the N-terminal region of the polyprotein by signal peptidase cleavages (15). In addition, processing in the C-terminal region of the capsid protein by a signal peptide peptidase leads to the generation of a mature capsid protein (32).

In the absence of a robust cell culture model for HCV, the analyses of the subcellular localization of HCV proteins have been performed with heterologous expression systems or in the context of HCV replicons (reviewed in references 15 and 33). Transient expression of HCV envelope glycoproteins with heterologous expression systems has shown that HCV envelope glycoproteins E1 and E2 assemble as a noncovalent heterodimer (11). Due to the presence of retention signals in the transmembrane domains of HCV envelope glycoproteins (8, 9), the glycoprotein heterodimer is mainly retained in the ER (17). However, in some expression systems, a fraction of HCV envelope glycoproteins has also been found to be located in the intermediate compartment and the *cis*-Golgi apparatus (12, 29, 37) and at the plasma membrane (3, 13, 24).

When expressed with heterologous expression systems or in the context of HCV replicons, the subcellular distribution of the capsid protein seems to be complex. Most of the protein is cytoplasmic where it is found both attached to the ER and at the surface of lipid droplets (for a review, see reference 31). The different extents to which the capsid protein is attached either to lipid droplets or membranes may be dependent on the amount of lipid droplets present in various cell types (22). In some conditions, a minor proportion of the capsid protein has also been found to be located in the nucleus (43). More recently, the capsid protein has also been found to colocalize with mitochondrial markers in Huh-7 cells containing a full-length HCV replicon (39).

Very recently, a cell culture model has been developed for HCV (26, 42, 44). This system is based on the transfection of the human hepatoma cell line Huh-7 with genomic RNA derived from a cloned viral genome. This culture system allows the production of virus that can be efficiently propagated in cell culture. Although a large amount of data has been accumulated on most HCV proteins during the past 15 years, the development of a cell culture system for HCV allows reinvestigation of the biological and biochemical properties of HCV proteins in a more relevant context. Here, we analyzed the

* Corresponding author. Mailing address: Unité Hépatite C, CNRS-UPR2511, Institut de Biologie de Lille, 1 Rue Calmette, BP447, 59021 Lille Cedex, France. Phone: (33) 3 20 87 11 60. Fax: (33) 3 20 87 12 01. E-mail: jean.dubuisson@ibl.fr.

† C.W. and J.D. contributed equally to this study.

subcellular localization of HCV structural proteins in Huh-7 cells infected with an infectious HCV clone. Our data show that, in infected cells, HCV glycoprotein heterodimer is retained in the ER and the capsid protein is detected in association with lipid droplets. However, in contrast to previous reports, no other subcellular localization was found for these proteins. In addition, no colocalization was observed between the glycoprotein heterodimer and the capsid protein in HCV-infected cells. Electron microscopy analyses identified membrane alterations in infected cells; however, dense elements compatible with the size and shape of a viral particle were seldom observed in HCV-infected cells.

MATERIALS AND METHODS

Cell culture and HCV production. Huh-7 human hepatoma cells (35) were grown in Dulbecco modified essential medium (Invitrogen) supplemented with 10% fetal bovine serum. The plasmid pJFH1 containing the full-length cDNA of JFH1 isolate, which belongs to subtype 2a (GenBank accession no. AB047639), has been described previously (42). To generate genomic HCV RNA, the plasmid pJFH1 was linearized at the 3′ end of the HCV cDNA by XbaI digestion. After treatment with mung bean nuclease, the linearized DNA was then purified and used as a template for in vitro transcription with the MEGAscript kit from Ambion. In vitro-transcribed RNA was delivered to cells by electroporation as described previously (25). Viral stocks were obtained by harvesting cell culture supernatants 1 week posttransfection. Secondary viral stocks of ca. 10^5 50% tissue culture infective doses/ml were obtained by additional amplifications on naive Huh-7 cells. Except for some electron microscopy studies, all of the experiments were done with Huh-7 cells infected with secondary viral stocks. For immunofluorescence studies, HCV-infected cells were treated with trypsin, seeded on coverslips, and grown for 3 to 4 days before processing for immunolabeling. Virus titration was performed as described previously (26) by immunostaining the cells with anti-E2 monoclonal antibody (MAb) 3/11.

Antibodies. Rat MAb 3/11 (19) was produced in vitro by using a MiniPerm apparatus (Heraeus) as recommended by the manufacturer. Mouse anti-E2 MAb AP33 has been previously described (7). Human anti-E1 MAb 1C4 (Innogenetics hybridoma clone IGH398) was obtained from a patient chronically infected with an HCV subtype 1b strain. This immunoglobulin G1 (IgG1) MAb has been mapped to the V3 region of E1 (amino acids 235 to 240) and has been shown to cross-react with E1 peptides from genotypes 1 to 6 (G. Maertens et al., unpublished data). Anti-capsid ACAP27 (28) and anti-NS3 (486D39) MAbs were kindly provided by J. F. Delagneau (Bio-Rad, France). Human anti-E2 MAb CBH5 (21), mouse anti-ERGIC-53 MAb (38), and anti-capsid MAb 6G7 (23) were kindly provided by S. Foung (Stanford University), H. P. Hauri (University of Basel, Basel, Switzerland) and H. B. Greenberg (Stanford University), respectively. Mouse anti-CD63 MAb TS63 (5) was a gift from E. Rubinstein (INSERM U602, Villejuif, France). Mouse anti-GM130 and anti-LAMP-1 MAbs were purchased from BD Biosciences. Rabbit antibodies to calnexin, calreticulin, and protein disulfide isomerase (PDI) were from Stressgen. Mouse anti-cytochrome *c* MAb 6H2.B4 was from Pharmingen. Guinea pig polyclonal antibody to human ADRP was purchased from Progen. Alexa 488-conjugated goat anti-rabbit, anti-mouse, anti-rat, or anti-human IgG, and isotype-specific Alexa488-conjugated goat anti-mouse IgG2a and Alexa555-conjugated goat anti-mouse IgG1 were purchased from Molecular Probes. Cy3-conjugated goat anti-mouse, anti-rat, or anti-guinea pig IgG were purchased from Jackson Immunoresearch (West Grove, PA).

Indirect immunofluorescence microscopy. Infected Huh-7 cells grown on 12-mm glass coverslips were fixed with 3% paraformaldehyde and then permeabilized with 0.1% Triton X-100 in phosphate-buffered saline (PBS). Both primary and secondary antibody incubations were carried out in PBS containing 10% goat serum for 30 min at room temperature. For double-label immunofluorescence with primary antibodies from different species, Cy3- and Alexa 488-conjugated secondary antibodies were used. For double-label immunofluorescence with anti-C MAb ACAP27 (IgG2a) and another mouse MAb (IgG1), isotype-specific Alexa 488-conjugated goat anti-mouse IgG2a and Alexa 555-conjugated goat anti-mouse IgG1 were used. Lipid droplets were stained with oil red O as described previously (22). Coverslips were mounted on slides by using Mowiol 4-88 (Calbiochem). Confocal microscopy was performed with an SP2 confocal laser-scanning microscope (Leica) using a ×100/1.4 numerical aperture oil immersion lens. Double-label immunofluorescence signals were sequentially collected by using single fluorescence excitation and acquisition settings to avoid crossover. Images were processed by using Adobe Photoshop software.

Cell surface labeling. Huh-7 cells infected by JFH1 virus or transfected with the plasmid phCMV-E1E2 (3) or phCMV-E1E2(LAL) (6), as well as control Huh-7 cells were used for cell surface labeling. Cells were incubated for 1 h on ice with the primary antibody. MAb 3/11 was used to detect E2 glycoprotein expressed at the cell surface. Experiments with a rabbit polyclonal anti-calnexin antiserum were carried out as a control for the lack of permeabilization of cell membranes. Cells were then washed three times with cold PBS, fixed with 3% paraformaldehyde. Alexa-488-conjugated goat anti-rat or rabbit secondary antibody incubation was carried out in PBS containing 10% goat serum for 30 min at room temperature.

Endoglycosidase digestions. Huh-7 cells infected by JFH1 virus or 393T cells transfected with the plasmid phCMV-E1E2 (3) were lysed with 0.5% Igepal CA-630 in TBS (50 mM Tris-Cl [pH 7.5], 150 mM NaCl). Cell lysates were used for immunoprecipitation with anti-E2 MAb AP33 as previously described (16). Immunoprecipitated proteins were eluted from protein-A Sepharose in 30 μl of dissociation buffer (0.5% sodium dodecyl sulfate [SDS] and 1% 2-mercaptoethanol) by boiling for 10 min. The protein samples were then divided into equal portions for digestion with either endo-β-*N*-acetylglucosaminidase H (endo H) or peptide:*N*-glycosidase F (PNGase F) and an undigested control. Digestions were carried out for 1 h at 37°C in the buffer provided by the manufacturer. Proteins were then analyzed by Western blotting.

Western blotting. After separation by SDS-polyacrylamide gel electrophoresis (PAGE), protein preparations were transferred to nitrocellulose membranes (Hybond-ECL; Amersham) by using a Trans-Blot apparatus (Bio-Rad) and revealed with a specific MAb, followed by the addition of goat anti-mouse or anti-rat immunoglobulin conjugated to peroxidase (Jackson Immunoresearch). The proteins of interest were revealed by enhanced chemiluminescence detection (ECL; Amersham) as recommended by the manufacturer.

Electron microscopy. For ultrastructural analysis, cells were fixed in 4% paraformaldehyde and 1% glutaraldehyde in 0.1 M phosphate buffer (pH 7.2) for 48 h. Cells were then washed in phosphate buffer, harvested, and postfixed with 1% osmium tetroxide for 1 h. They were then dehydrated in a graded acetone series, and cell pellets were embedded in Epon resin, which was allowed to polymerize for 24 h at 60°C. Ultrathin sections were cut on an ultramicrotome (Reichert, Heidelberg, Germany), collected on copper grids and stained with 1% uranyl acetate–1% lead citrate. The grids were then observed with a 1010 XC electron microscope (JEOL, Tokyo, Japan).

RESULTS

The glycoprotein heterodimer is located in the ER of HCV-infected cells. Efficient viral replication of JFH1 isolate was obtained by amplification on naive Huh-7 cells with virus titers of ca. 10^5 50% tissue culture infective doses/ml. This allowed us to reinvestigate the subcellular localization of HCV structural proteins in the context of an infectious cycle. The subcellular distribution of HCV envelope glycoproteins was examined by confocal immunofluorescence microscopy. To define the intracellular localization of E1 and E2 during HCV infection, we looked for antibodies that recognize the glycoproteins of the JFH1 strain in immunofluorescence analyses. Huh-7 cells were either mock infected or infected with HCV, grown on glass coverslips, fixed with paraformaldehyde, and processed for indirect immunofluorescence with various anti-E1 or anti-E2 antibodies. A large panel of antibodies that were raised against HCV glycoproteins of genotype 1 was screened. However, only anti-E1 MAb 1C4 and anti-E2 MAbs 3/11, AP33, and CBH5 were found to specifically label HCV-infected Huh-7 cells, but not naive cells in indirect immunofluorescence. Immunoblot analysis confirmed that MAb 1C4 recognizes the glycoprotein E1 and that MAbs 3/11 and AP33 recognize the glycoprotein E2 of the JFH1 strain (Fig. 1A and data not shown).

HCV-infected cells stained with MAbs 1C4, 3/11, or AP33 displayed a pattern of specific fluorescence in a network of

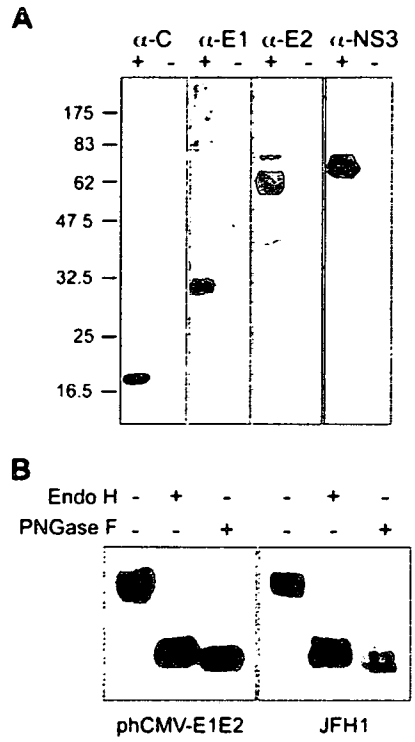

FIG. 1. Expression of HCV proteins in HCV-infected cells. (A) Analysis of the expression of HCV proteins C, E1, E2, and NS3 by Western blotting. Lysates of naive (−) or HCV-infected (+) cells were separated by SDS-PAGE and revealed by Western blotting with MAbs ACAP27 (anti-C), 1C4 (anti-E1), 3/11 (anti-E2), and 486D39 (anti-NS3). The sizes of protein molecular mass markers are indicated on the right (in kilodaltons). (B) Analyses of the glycans associated with HCV glycoprotein E2. Lysates of HCV-infected cells Huh-7 cells (JFH1) or 293T cells transfected with a plasmid expressing HCV envelope glycoproteins (phCMV-E1E2) were immunoprecipitated with anti-E2 MAb AP33. The immunoprecipitates were treated or not treated with endo H or PNGase F. Proteins were then separated by SDS-PAGE and revealed by Western blotting with the anti-E2 MAb 3/11.

cytoplasmic membranes and the nuclear envelope (Fig. 2). A very similar pattern of staining was also observed with MAb CBH5 (not shown). As expected, since they assemble as a heterodimer during their folding (11), E1 and E2 glycoproteins colocalized (Fig. 2). Interactions between E1 and E2 of JFH1 strain were confirmed by coimmunoprecipitation (data not shown). To further define the intracellular localization of HCV glycoprotein heterodimer in infected cells, double-label immunofluorescence experiments were carried out with an anti-E2 MAb. HCV-infected cells grown on glass coverslips were incubated with MAb 3/11, together with antibodies specific for various intracellular compartments. Within the secretory pathway, E2 colocalized predominantly with proteins of the ER, including calnexin (Fig. 2, calnexin), calreticulin, and PDI (not shown). In contrast to other studies (29, 37), E2 did not colocalize with the marker of the intermediate compartment ERGIC-53 (Fig. 2, ergic53) or with the Golgi marker GM130 (Fig. 2, GM130). In addition, E2 did not colocalize with markers of the endocytic pathway, such as EEA-1, a protein localized in early endosomes; CD63, a marker of multivesicular endosomes (not shown); or LAMP-1, a marker of late endosomes and lysosomes (Fig. 2, lamp-1). It is worth noting that we did not detect any change in the subcellular localization of HCV glycoprotein heterodimer when analyzed at different times posttransfection (48, 72, and 96 h) or postinfection (48 and 72 h). These findings demonstrate that the glycoprotein heterodimer localizes predominantly to the ER in HCV-infected cells, and they are in agreement with previous data obtained in the context of the expression of the full-length HCV polyprotein (17).

The glycoprotein heterodimer is not expressed at the plasma membrane of HCV-infected cells. Recently, it has been shown that, in some transient expression systems, a fraction of HCV envelope glycoproteins can also be detected at the plasma membrane (3, 13, 24). We therefore investigated whether HCV glycoprotein heterodimer can leave the ER and be exported to the plasma membrane in the context of HCV-infected cells.

To determine whether a fraction of HCV glycoprotein heterodimer has left the ER compartment, we analyzed whether the glycans associated with HCV glycoprotein E2 have been modified by Golgi enzymes by evaluating their sensitivity to endo H treatment. Resistance to digestion with endo H is indicative that glycoproteins have moved from the ER to at least the medial and *trans*-Golgi, where complex sugars are formed. PNGase F treatment, which removes all types of N-linked glycans, was used as a control of deglycosylation. As shown in Fig. 1B, the glycoprotein E2 remained endo H sensitive in HCV-infected cells, whereas a faint endo H-resistant band was observed for E2 expressed in cells transfected with a plasmid expressing HCV envelope glycoproteins. As previously observed (14), due to the presence of a residual *N*-acetylglucosamine at each glycosylation position after endo H treatment, the endo H-treated E2 migrated slightly more slowly than the PNGase F-treated protein. An additional slightly slower migrating band was detected for both PNGase F- and endo H-treated proteins (Fig. 1B). Such a partial resistance to PNGase F treatment has already been observed for truncated forms of HCV glycoprotein E2, as well as for E1 expressed in HCV pseudotyped particles (36).

Cell surface expression was determined by surface labeling using the anti-E2 MAb 3/11. Although an E2 staining was clearly detected in HCV-infected cells treated with Triton X-100 (Fig. 3, compare panels A and B), no E2 protein was detected at the cell surface (Fig. 3C). Interestingly, E2 was detected at the plasma membrane of Huh-7 cells transfected with a plasmid expressing HCV envelope glycoproteins of genotype 1a (Fig. 3E). It is worth noting that there was a correlation between the level of expression and cell surface detection (data not shown). In addition, as previously observed (6, 10), the level of expression of E2 at the cell surface was higher when the charged residues in the transmembrane domain of E2 were mutated (Fig. 3F). When expressed from a plasmid, the expression level of HCV envelope glycoproteins of JFH1 isolate was approximately 15 times higher than in the context of HCV-infected cells; however, they were not detected above background at the cell surface (data not shown), indicating that there might be some differences between isolates or subtypes for cell surface expression. Altogether, these data indicate that HCV glycoprotein heterodimer does not accumulate at the plasma membrane in HCV-infected cells.

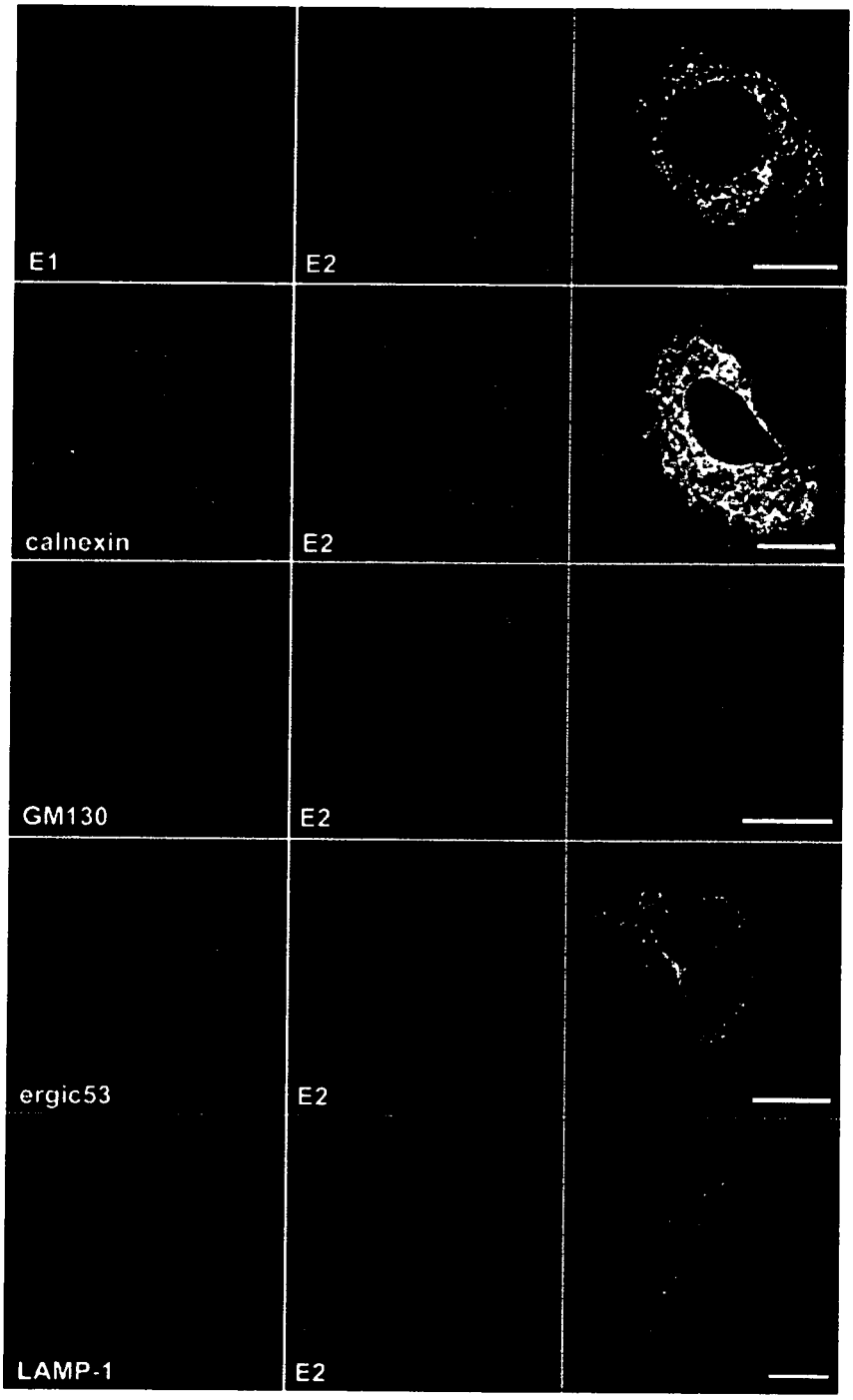

FIG. 2. Confocal immunofluorescence analysis of the intracellular distribution of HCV glycoproteins. Infected cells grown on coverslips were fixed and processed for double-label immunofluorescence for E1, E2, and the following cellular markers: calnexin, a chaperone of the ER; GM130, a Golgi matrix protein; ERGIC-53, a marker of the ER-to-Golgi intermediate compartment; or LAMP-1, a marker of late endosomes and lysosomes. Anti-E2 mouse MAb AP33 was used for the colocalization with E1. For the other experiments, E2 was revealed with the rat MAb 3/11. Representative confocal images of individual cells are shown with the merge images in the right column. Bar, 20 μm.

Intracellular localization of the capsid protein in HCV-infected cells. To detect the capsid protein, we used the 6G7 (23) and ACAP27 (28) antibodies, two mouse MAbs that recognize two different epitopes located at amino acids 29 to 39 and amino acids 40 to 53, respectively. Consistent with the high levels of sequence conservation among core proteins from different genotypes, both MAbs gave positive signals in Huh-7 cells infected with JFH1 virus (Fig. 4 and data not shown).

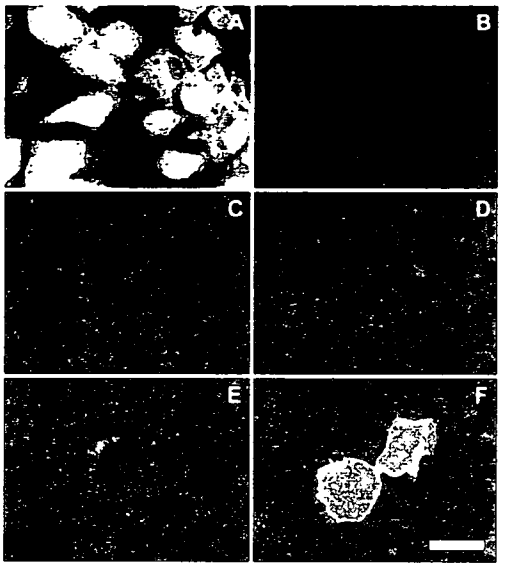

FIG. 3. Cell surface expression of HCV glycoprotein E2. Naive (B and D) or infected (A and C) Huh-7 cells grown on coverslips were labeled with the anti-E2 MAb 3/11. A set of cells was fixed with 3% paraformaldehyde and processed for immunofluorescence labeling after permeabilization with Triton X-100 (A and B). Cell surface labeling (C, D, E, and F) was carried out on ice with MAb 3/11 before the fixation with 3% paraformaldehyde and the incubation with Alexa488-labeled secondary antibody. Huh-7 cells transfected with a plasmid expressing wild-type HCV envelope glycoproteins (phCMV-E1E2; panel E) or HCV envelope glycoproteins containing a mutation of the charged residues in the transmembrane domain of E2 [phCMV-E1E2(LAL); panel F] were used as controls of cell surface expression of E2. All images were acquired and processed with the same settings. Bar, 50 μm.

Immunoblot analysis confirmed that they recognize the core protein of the JFH1 strain (Fig. 1 and data not shown). The capsid protein migrated as a single species with an apparent molecular mass of 21 kDa, which most likely corresponded to the processed form of the capsid protein from which the signal sequence of E1 has been removed.

HCV-infected cells incubated with either anti-C protein MAbs displayed very similar patterns of bright fluorescence strictly limited to the cell cytoplasm and frequently concentrated in the perinuclear region (Fig. 4 and data not shown). In contrast, naive Huh-7 cells were not stained, indicating the specificity of the labeling (data not shown). In the perinuclear region, the staining pattern often displayed ring-like structures (Fig. 4). Double-label immunofluorescence experiments were performed in order to define the intracellular localization of the C protein. We did not observe, in contrast to E2, any colocalization between C and markers of the ER, such as calnexin (Fig. 4), calreticulin, or PDI (data not shown). In contrast to another report analyzing the subcellular localization in a cell line inducibly expressing HCV structural proteins (29), the perinuclear area containing the C protein was not localized in the Golgi complex and did not colocalize with the marker of the intermediate compartment (Fig. 4). In addition, no colocalization was observed with markers of the endocytic pathway, such as EEA-1 or Lamp-1 (data not shown).

Expression with heterologous expression systems or in the context of a full-length HCV replicon has shown that HCV capsid protein can associate with lipid droplets (1, 22, 37). We therefore analyzed whether the C protein expressed in HCV-infected cells would colocalize with lipid droplets. When lipid droplets were labeled with oil red O, an association between the C protein and lipid droplets was clearly observable. However, in contrast to previous reports, a fraction of the C protein was not directly associated with the lipid droplets, and the pattern of labeling was consistent with this fraction of the C protein being localized in a membranous compartment that is associated with the lipid droplets (see zoomed inset in Fig. 4). It is worth noting that we did not detect any change in the subcellular localization of the C protein when analyzed at different times posttransfection (48, 72, and 96 h) or postinfection (48 and 72 h).

To confirm the association of C with lipid droplets, double-label immunofluorescence experiments were carried out with an antibody to ADRP, which is a marker of the cytosolic pool of lipid droplets. In most infected cells, C and ADRP displayed an extensive colocalization (Fig. 4). At a higher magnification, C and ADRP were often concentrated on different parts of single lipid droplet-like ring structures (Fig. 4 ADRP, inset). In addition, no competition between both proteins for the association to lipid droplets was observed, as judged by the relative levels of ADRP and C immunoreactive signals in individual cells (not shown).

It has been shown that a fraction of the C protein expressed with heterologous systems can be located in the nucleus (43). However, we did not detect such a subcellular localization in HCV-infected cells (Fig. 4). Other reports have also proposed that a fraction of the C protein could be associated with mitochondria (39) and/or an Apo-AII-positive compartment (1). However, double-label immunofluorescence experiments in HCV-infected Huh-7 cells did not confirm the colocalization of the C protein with Apo-AII or mitochondria (data not shown). The detection of the capsid protein in the nucleus or the mitochondria as observed in other reports is potentially due to protein overexpression, to saturation of fluorescence signals, or to the absence of particle formation.

Altogether, our results show that the capsid protein is localized at the surface of lipid droplets and in a membranous compartment that is associated with the lipid droplets.

Relative intracellular localization of HCV glycoprotein heterodimer, capsid protein, and NS3. HCV nonstructural proteins NS3 to NS5B are the viral components of HCV replication complex (2), and they have been shown to colocalize in Huh-7 cells containing a subgenomic replicon (20). In addition, due to the presence of NS4B, the expression of HCV nonstructural proteins induces the formation of a virus-induced structure designated the membranous web (18). HCV structural and nonstructural proteins have been shown to colocalize with the membranous web (18), suggesting that the replication and assembly factories might be located within the same virus-induced organelle. We therefore analyzed whether HCV glycoprotein heterodimer would colocalize with the C protein and whether the localization of structural proteins would overlap that of nonstructural proteins. We chose to use an anti-NS3 antibody to detect one of the components of the replication complex. Immunofluorescence with the anti-NS3 MAb was positive on HCV-infected cells (Fig. 5) and negative on control cells (data not shown). Immunoblot analysis confirmed that the

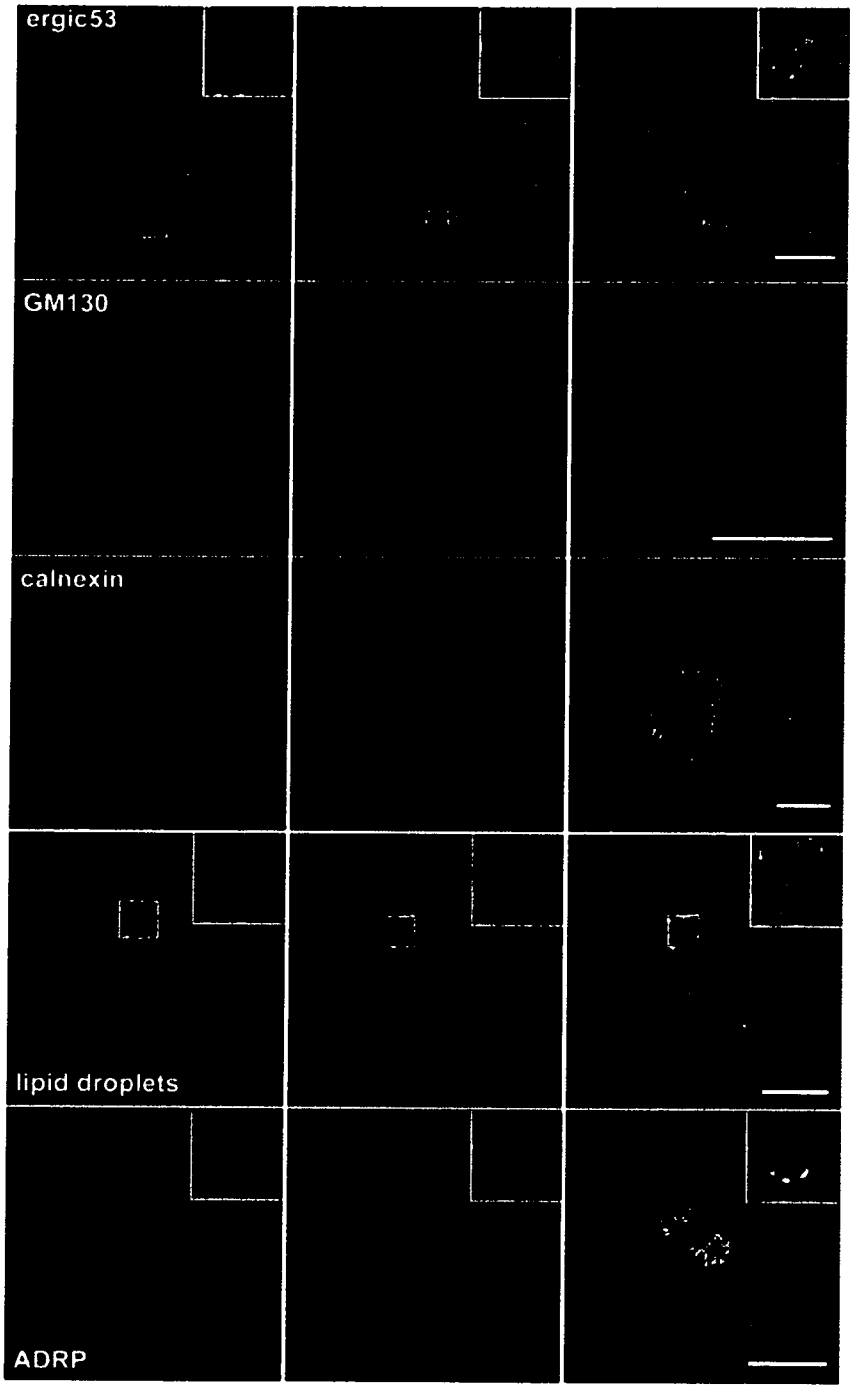

FIG. 4. Confocal immunofluorescence analysis of the intracellular distribution of the capsid protein. Infected cells grown on coverslips were fixed and processed for double-label immunofluorescence for C (green) and the following cellular markers (red): ERGIC-53, a marker or the ER-to-Golgi intermediate compartment; GM130, a Golgi matrix protein; calnexin, a chaperone of the ER; or ADRP, a marker of the cytosolic pool of lipid droplets. Lipid droplets were stained with oil red O. Representative confocal images of individual cells are shown with the merge images in the right column. Insets display zoomed views of the indicated area. Bar, 20 μm.

anti-NS3 MAb recognizes the NS3 protein of the JFH1 strain (Fig. 1A).

Double-label immunofluorescence experiments with anti-C and anti-E2 antibodies did not show any colocalization between C and E2 (Fig. 5). This is in agreement with the colocalization of E2 with ER markers and the absence of colocalization between the C protein and ER makers (Fig. 2 and 4). In contrast, a partial colocalization was observed between the

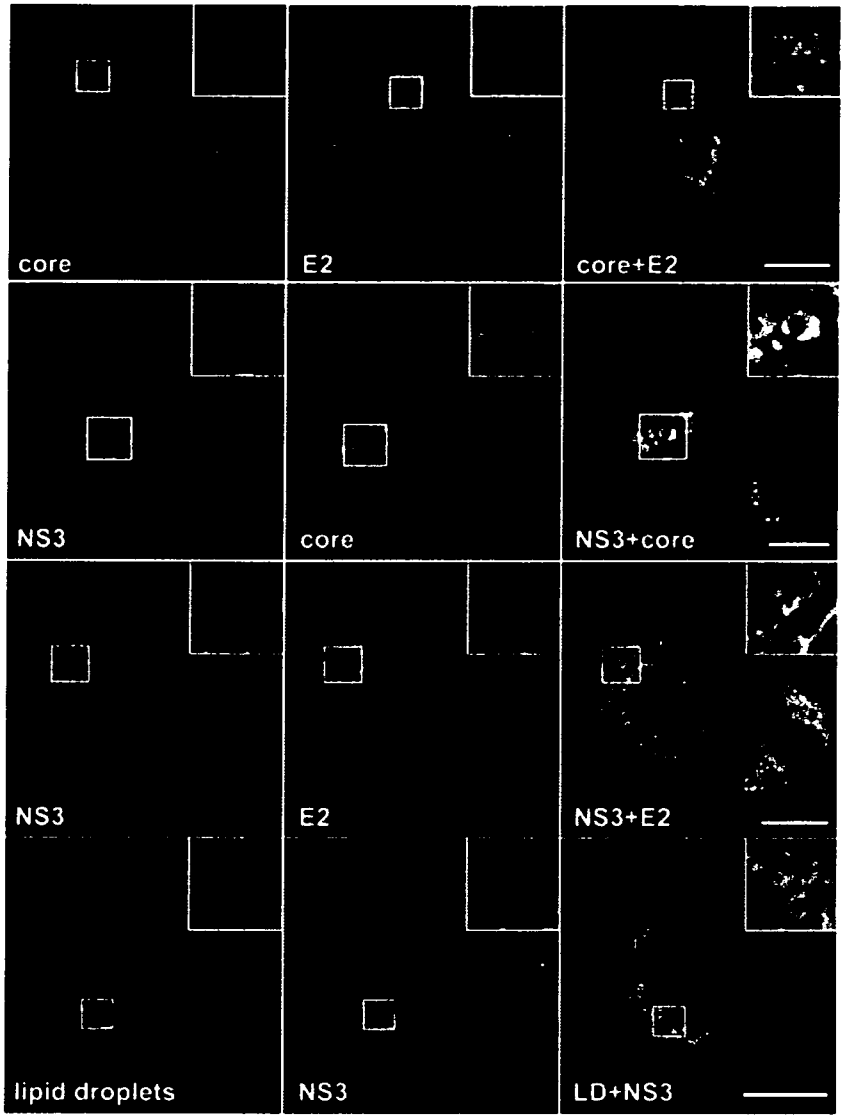

FIG. 5. Relative intracellular localization of HCV proteins C, E2, and NS3 analyzed by confocal immunofluorescence. Infected cells grown on coverslips were fixed and processed for double-label immunofluorescence for C and E2 (top row), NS3 and C (middle row), or NS3 and E2 (bottom row). Lipid droplets were stained with oil red O. Representative confocal images of individual cells are shown with the merge images in the right column. Insets display zoomed views of the indicated area. Bar, 20 μm.

C protein and NS3 and between E2 glycoprotein and NS3 (Fig. 5). NS3 displayed an ER-like pattern of immunofluorescence, which colocalized partially with E2. In addition, in a number of cells NS3 labeling was often more intense in the perinuclear area, where it partially colocalized with the C protein (Fig. 5). Interestingly, when lipid droplets were labeled with oil red O, the NS3 protein was also found around lipid droplets (Fig. 5).

Ultrastructural aspects of HCV-infected cells. To identify ultrastructural modifications induced by JFH1 replication and the potential presence of viral particles, we investigated Huh-7 cells containing replicative JFH1 genome by electron microscopy. In a first set of experiments, we used Huh-7 cells transfected with JFH1 genomic RNA to have virtually all of the cells containing a replicative virus (Fig. 6). We then confirmed our observations on HCV-infected cells (data not shown). Lipid droplets were often observed in cells containing replicative JFH1 genome (Fig. 6A); however, there is no evidence that lipid droplets accumulate more in HCV-infected cells than in control naive Huh-7 cells. A membranous web composed of small vesicles was also found in many Huh-7 cells containing replicative JFH1 genome (Fig. 6B) but not in naive cells (data not shown). Figure 6C shows a membranous web at higher magnification. This structure was similar to the membranous web previously identified in U-2 OS human osteosarcoma-derived cell lines inducibly expressing the HCV polyprotein and in Huh-7 cells harboring a subgenomic HCV replicon (18, 20). Virus-like particles were never found in the membranous web. Some electron-dense elements compatible in size and

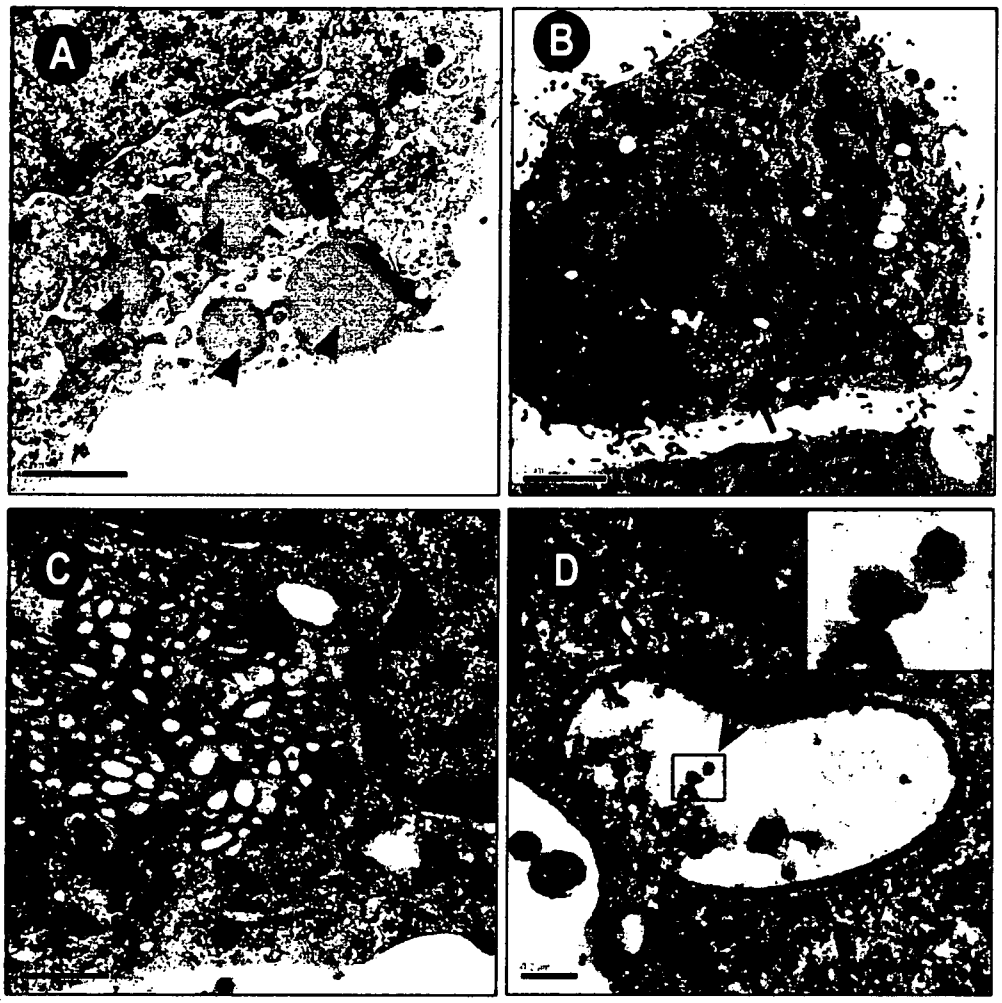

FIG. 6. Membrane alterations in Huh-7 cells containing replicative JFH1 genome visualized by electron microscopy. (A) Cell containing several lipid droplets (arrows). Bar, 2 μm. (B) Low-power overview showing a membranous web (arrow). Bar, 2 μm. (C) Higher magnification of the membranous web. Bar, 0.5 μm. (D) Small cisternae containing electron-dense elements compatible in size and shape with virus-like or core particles (arrows). Bar, 0.2 μm. Inset displays zoomed view of the indicated area.

shape with virus-like or core particles were sometimes found in small cisternae of Huh7 cells containing replicative JFH1 genome (Fig. 6D). These particles were smaller and more regular than the glycogen particles that are abundantly present in the Huh7 cells, but they were rare and their relationship with viral structures remains to be determined.

DISCUSSION

The recent development of a cell culture model for HCV (26, 42, 44) allows the production of virus that can be efficiently propagated in cell culture. This cell culture system has allowed us to reinvestigate the subcellular localization of HCV structural proteins in the context of an infectious cycle. Here, we showed that, in infected cells, HCV glycoprotein heterodimer is retained in the ER and the capsid protein is detected in association with lipid droplets. In contrast to previous reports, the glycoprotein heterodimer and the capsid protein were not detected in other subcellular localizations. Interestingly, electron microscopy analyses identified membrane alterations in infected cells. However, dense elements compatible with viral particles were seldom observed in HCV-infected cells.

HCV glycoprotein heterodimer is retained in the ER in infected cells. This is in agreement with several studies with heterologous expression systems containing HCV envelope glycoproteins or in the context of the full-length HCV polyprotein (11, 14, 17). Indeed, ER localization signals have been identified in the transmembrane domains of E1 and E2 (8, 9). Other studies have, however, shown that a fraction of HCV envelope glycoproteins can also be found in the ERGIC and in the *cis*-Golgi apparatus (29, 37). The presence of HCV glycoprotein heterodimer in these compartments is potentially due to protein overexpression, to saturation of fluorescence signals, or to the absence of particle formation. Indeed, such localization in the ERGIC and in the *cis*-Golgi apparatus was not observed in HCV-infected cells.

HCV glycoprotein heterodimer is not exported to the plasma membrane in infected cells. In some conditions of expression, a small fraction of HCV envelope glycoproteins

has been shown to accumulate at the plasma membrane, and this led to the development of a system to pseudotype retroviral particles with HCV envelope proteins that has proven crucial for studying HCV entry (3, 13, 24, 36). However, cell surface expression of HCV glycoprotein heterodimer is not observed in HCV-infected cells, and export at the plasma membrane with the heterologous system might be due to the accumulation of small amounts of glycoproteins escaping the ER retention machinery due to saturation of this mechanism. It is worth noting that in the case of JFH1 envelope glycoproteins expressed from a plasmid, the glycoproteins were not detected at the cell surface, suggesting that there might also be some differences between isolates or subtypes for the subcellular localization of the envelope glycoproteins.

The capsid protein is detected in association with lipid droplets in infected cells. This is in agreement with other studies using heterologous expression systems or in the context of a full-length HCV replicon (1, 22, 37). However, in contrast to these studies, a fraction of the C protein was not directly associated with the lipid droplets, and this suggests a localization of the C protein in a membranous compartment that is associated with the lipid droplets, in addition to the localization of another fraction of the C protein at the surface of lipid droplets. Lipid droplets consist of a core of triglycerides and cholesterol esters surrounded by a monolayer of phospholipids and a proteinaceous coat (34). The most likely mechanism by which triglycerides and cholesterol esters end up in cytosolic lipid particles is that they first accumulate between the leaflets of the ER lipid bilayer and, after reaching a critical size, a lipid droplet would bud off the cytosolic side of the ER membrane (40). However, some droplets can remain physically connected to the ER membrane (4). From our immunolocalization study, it can be suggested that the C protein localizes at the site of lipid droplet formation. Although the C protein was not found to colocalize with the markers of ER membranes in HCV-infected cells, its localization at the potential site of lipid droplet formation suggests that the C protein does not associates with the rough ER but might attach to a subcompartment of the ER, which is potentially the smooth ER. We can also not exclude that this subcompartment corresponds to cytoplasmic raft microdomains that have been recently reported to contain the C protein (30).

The absence of colocalization between the C protein and classical markers of the ER compartment contrasts with some reports indicating that the C protein interacts with rough ER membranes (for a review, see reference 31). Interestingly, it has been reported that the traffic between rough ER membranes, the site of capsid protein synthesis, and lipid droplets is regulated by signal peptide peptidase cleavage in the C-terminal region of the capsid protein (32). It is therefore likely that in the context of HCV-infected cells, transport of the C protein to the site of lipid droplet assembly is rapid due to rapid cleavage by the signal peptide peptidase. It has also been previously reported that the different extents to which the capsid protein is associated with lipid droplets or rough ER membranes may be dependent on the amount of lipid droplets present in various cell types (22). Since HCV-infected cells accumulate lipid droplets, they provide the conditions for a shift toward accumulation of the C protein in association with lipid droplets.

The significance of the association of HCV capsid protein to a lipid droplet related compartment is not understood. Since the capsid protein is a major component of the viral particle, one might expect that this interaction plays a role in some step of virion morphogenesis. It is possible that the sites of lipid droplet formation provide a platform for nucleocapsid assembly by concentrating viral and/or cellular components that are necessary for the assembly of the nucleocapsid and/or by excluding those that inhibit this process. Interestingly, NS3 appears to partially colocalize with C in this compartment.

The glycoprotein heterodimer and the capsid protein do not colocalize in HCV-infected cells. Since the glycoprotein heterodimer and the capsid protein are the protein components of HCV particle, one would expect that these proteins would accumulate at the same site for virion assembly. Indeed, production of infectious virus particles likely requires spatially and temporally coordinated interactions of components that make up an infectious virion. The absence of colocalization between the glycoprotein heterodimer and the capsid protein would suggest that particle assembly is a two-step process involving nucleocapsid assembly, followed by a budding process occurring in two separate compartments. However, in the absence of sufficient data, it would be premature to generate a model of HCV particle assembly. To have a better idea of HCV morphogenesis, one would need to analyze the subcellular localization of HCV structural proteins in living cells. This would help elucidate the dynamics of the protein interactions between different cellular compartments.

Some viruses require membrane surfaces on which to assemble their replication complex. Such interactions have been well documented for positive-strand RNA viruses (41). In the case of HCV, a structure called membranous web has been previously identified in cell lines inducibly expressing the HCV polyprotein (18). In addition, such structures have also been shown to contain HCV RNA replication complex in cells harboring subgenomic replicons (20). Interestingly, a membranous web composed of small vesicles was also found in HCV-infected cells. However, these structures did not contain any virus-like particles, suggesting that HCV particle assembly does not occur in the membranous web.

The recent development of a cell culture model for HCV has allowed us to investigate for the first time the subcellular localization of HCV structural proteins in the context of a replicative and assembly competent virus. Interestingly, our data indicate that investigating the properties of HCV proteins expressed in heterologous systems do not necessarily reflect those that they have in the context of an infectious cycle. In conclusion, the cell culture system for HCV warrants reinvestigation of the biochemical and biological properties of HCV proteins in order to better understand their functional significance in the context of active viral replication and morphogenesis.

ACKNOWLEDGMENTS

We thank André Pillez, Sophana Ung, and Sylvie Trassard for technical assistance. We are grateful to J. F. Delagneau, S. Foung, H. P. Hauri, H. B. Greenberg, E. Rubinstein, F. L. Cosset, and B. Bartosch for providing reagents. The data presented here were generated with the help of the Imaging Core Facility of the Calmette Campus and the Electron Microscopy Facility of the University of Tours.

This study was supported by EU grant QLRT-2001-01329 and grants from the Agence Nationale de Recherche sur le SIDA et les Hépatites Virales (ANRS) and INSERM ATC-Hépatite C. Some of the authors were supported by fellowships from the French Ministry of Research (F.H.), the ANRS (D.D. and E.B.), and the CNRS (C.V.). T.W. was partly supported by grants from the Ministry of Health, Labor, and Welfare of Japan; the Program for Promotion of Fundamental Studies in Health Sciences of the National Institute of Biomedical Innovation (NIBIO); and Research on Health Sciences focusing on Drug Innovation of the Japan Health Sciences Foundation. J.D. is an international scholar of the Howard Hughes Medical Institute.

REFERENCES

1. **Barba, G., F. Harper, T. Harada, M. Kohara, S. Goulinet, Y. Matsuura, G. Eder, Z. Schaff, M. J. Chapman, T. Miyamura, and C. Brechot.** 1997. Hepatitis C virus core protein shows a cytoplasmic localization and associates to cellular lipid storage droplets. Proc. Natl. Acad. Sci. USA **94**:1200–1205.
2. **Bartenschlager, R., M. Frese, and T. Pietschmann.** 2004. Novel insights into hepatitis C virus replication and persistence. Adv. Virus Res. **63**:71–180.
3. **Bartosch, B., J. Dubuisson, and F. L. Cosset.** 2003. Infectious hepatitis C pseudo-particles containing functional E1E2 envelope protein complexes. J. Exp. Med. **197**:633–642.
4. **Blanchette-Mackie, E. J., N. K. Dwyer, T. Barber, R. A. Coxey, T. Takeda, C. M. Rondinone, J. L. Theodorakis, A. S. Greenberg, and C. Londos.** 1995. Perilipin is located on the surface layer of intracellular lipid droplets in adipocytes. J. Lipid. Res. **36**:1211–1226.
5. **Charrin, S., F. Le Naour, M. Oualid, M. Billard, G. Faure, S. M. Hanash, C. Boucheix, and E. Rubinstein.** 2001. The major CD9 and CD81 molecular partner: identification and characterization of the complexes. J. Biol. Chem. **276**:14329–14337.
6. **Ciczora, Y., N. Callens, C. Montpellier, B. Bartosch, F. L. Cosset, A. Op De Beeck, and J. Dubuisson.** 2005. Contribution of the charged residues of HCV glycoprotein E2 transmembrane domain to the functions of E1E2 heterodimer. J. Gen. Virol. **86**:2793–2798.
7. **Clayton, R. F., A. Owsianka, J. Aitken, S. Graham, D. Bhella, and A. H. Patel.** 2002. Analysis of antigenicity and topology of E2 glycoprotein present on recombinant hepatitis C virus-like particles. J. Virol. **76**:7672–7682.
8. **Cocquerel, L., S. Duvet, J.-C. Meunier, A. Pillez, R. Cacan, C. Wychowski, and J. Dubuisson.** 1999. The transmembrane domain of hepatitis C virus glycoprotein E1 is a signal for static retention in the endoplasmic reticulum. J. Virol. **73**:2641–2649.
9. **Cocquerel, L., J.-C. Meunier, A. Pillez, C. Wychowski, and J. Dubuisson.** 1998. A retention signal necessary and sufficient for endoplasmic reticulum localization maps to the transmembrane domain of hepatitis C virus glycoprotein E2. J. Virol. **72**:2183–2191.
10. **Cocquerel, L., C. Wychowski, F. Minner, F. Penin, and J. Dubuisson.** 2000. Charged residues in the transmembrane domains of hepatitis C virus glycoproteins play a key role in the processing, subcellular localization, and assembly of these envelope proteins. J. Virol. **74**:3623–3633.
11. **Deleersnyder, V., A. Pillez, C. Wychowski, K. Blight, J. Xu, Y. S. Hahn, C. M. Rice, and J. Dubuisson.** 1997. Formation of native hepatitis C virus glycoprotein complexes. J. Virol. **71**:697–704.
12. **De Martynoff, G., A. Venneman, and G. Maertens.** 1997. Analysis of post-translational modifications of HCV structural proteins by using the vaccinia virus expression system, p. 39–44. *In* M. Rizzetto, R. H. Purcell, and H. Gerin (ed.), Viral hepatitis and liver disease. Minerva Medica, Turin, Italy.
13. **Drummer, H. E., A. Maerz, and P. Poumbourios.** 2003. Cell surface expression of functional hepatitis C virus E1 and E2 glycoproteins. FEBS Lett. **546**:385–390.
14. **Dubuisson, J., H. H. Hsu, R. C. Cheung, H. B. Greenberg, D. G. Russell, and C. M. Rice.** 1994. Formation and intracellular localization of hepatitis C virus envelope glycoprotein complexes expressed by recombinant vaccinia and Sindbis viruses. J. Virol. **68**:6147–6160.
15. **Dubuisson, J., F. Penin, and D. Moradpour.** 2002. Interaction of hepatitis C virus proteins with host cell membranes and lipids. Trends Cell. Biol. **12**: 517–523.
16. **Dubuisson, J., and C. M. Rice.** 1996. Hepatitis C virus glycoprotein folding: disulfide bond formation and association with calnexin. J. Virol. **70**:778–786.
17. **Duvet, S., L. Cocquerel, A. Pillez, R. Cacan, A. Verbert, D. Moradpour, C. Wychowski, and J. Dubuisson.** 1998. Hepatitis C virus glycoprotein complex localization in the endoplasmic reticulum involves a determinant for retention and not retrieval. J. Biol. Chem. **273**:32088–32095.
18. **Egger, D., B. Wölk, R. Gosert, L. Bianchi, H. E. Blum, D. Moradpour, and K. Bienz.** 2002. Expression of hepatitis C virus proteins induces distinct membrane alterations including a candidate viral replication complex. J. Virol. **76**:5974–5984.
19. **Flint, M., C. Maidens, L. D. Loomis-Price, C. Shotton, J. Dubuisson, P. Monk, A. Higginbottom, S. Levy, and J. A. McKeating.** 1999. Characterization of hepatitis C virus E2 glycoprotein interaction with a putative cellular receptor, CD81. J. Virol. **73**:6235–6244.
20. **Gosert, R., D. Egger, V. Lohmann, R. Bartenschlager, H. E. Blum, K. Bienz, and D. Moradpour.** 2003. Identification of the hepatitis C virus RNA replication complex in Huh-7 cells harboring subgenomic replicons. J. Virol. **77**:5487–5492.
21. **Hadlock, K. G., R. E. Lanford, S. Perkins, J. Rowe, Q. Yang, S. Levy, P. Pileri, S. Abrignani, and S. K. Foung.** 2000. Human monoclonal antibodies that inhibit binding of hepatitis C virus E2 protein to CD81 and recognize conserved conformational epitopes. J. Virol. **74**:10407–10416.
22. **Hope, R. G., and J. McLauchlan.** 2000. Sequence motifs required for lipid droplet association and protein stability are unique to the hepatitis C virus core protein. J. Gen. Virol. **81**:1913–1925.
23. **Hsu, H. H., M. Donets, H. B. Greenberg, and S. M. Feinstone.** 1993. Characterization of hepatitis C virus structural proteins with a recombinant baculovirus expression system. Hepatology **17**:763–771.
24. **Hsu, M., J. Zhang, M. Flint, C. Logvinoff, C. Cheng-Mayer, C. M. Rice, and J. A. McKeating.** 2003. Hepatitis C virus glycoproteins mediate pH-dependent cell entry of pseudotyped retroviral particles. Proc. Natl. Acad. Sci. USA **100**:7271–7276.
25. **Kato, T., T. Date, M. Miyamoto, A. Furusaka, K. Tokushige, M. Mizokami, and T. Wakita.** 2003. Efficient replication of the genotype 2a hepatitis C virus subgenomic replicon. Gastroenterology **125**:1808–1817.
26. **Lindenbach, B. D., M. J. Evans, A. J. Syder, B. Wolk, T. L. Tellinghuisen, C. C. Liu, T. Maruyama, R. O. Hynes, D. R. Burton, J. A. McKeating, and C. M. Rice.** 2005. Complete replication of hepatitis C virus in cell culture. Science **309**:623–626.
27. **Lindenbach, B. D., and C. M. Rice.** 2001. *Flaviviridae*: the viruses and their replication, p. 991–1042. *In* D. M. Knipe and P. M. Howley (ed.), Fields virology, 4th ed. Lippincott/The Williams & Wilkins Co., Philadelphia, Pa.
28. **Maillard, P., K. Krawczynski, J. Nitkiewicz, C. Bronnert, M. Sidorkiewicz, P. Gounon, J. Dubuisson, G. Faure, R. Crainic, and A. Budkowska.** 2001. Nonenveloped nucleocapsids of hepatitis C virus in the serum of infected patients. J. Virol. **75**:8240–8250.
29. **Martire, G., A. Viola, L. Iodice, L. V. Lotti, R. Gradini, and S. Bonatti.** 2001. Hepatitis C virus structural proteins reside in the endoplasmic reticulum as well as in the intermediate compartment/*cis*-Golgi complex region of stably transfected cells. Virology **280**:176–182.
30. **Matto, M., C. M. Rice, B. Aroeti, and J. S. Glenn.** 2004. Hepatitis C virus core protein associates with detergent-resistant membranes distinct from classical plasma membrane rafts. J. Virol. **78**:12047–12053.
31. **McLauchlan, J.** 2000. Properties of the hepatitis C virus core protein: a structural protein that modulates cellular processes. J. Viral Hepat. **7**:2–14.
32. **McLauchlan, J., M. K. Lemberg, R. G. Hope, and B. Martoglio.** 2002. Intramembrane proteolysis promotes trafficking of hepatitis C virus core protein to lipid droplets. EMBO J. **21**:3980–3988.
33. **Moradpour, D., R. Gosert, D. Egger, F. Penin, H. E. Blum, and K. Bienz.** 2003. Membrane association of hepatitis C virus nonstructural proteins and identification of the membrane alteration that harbors the viral replication complex. Antivir. Res. **60**:103–109.
34. **Murphy, D. J., and J. Vance.** 1999. Mechanisms of lipid-body formation. Trends Biochem. Sci. **24**:109–115.
35. **Nakabayashi, H., K. Taketa, K. Miyano, T. Yamane, and J. Sato.** 1982. Growth of human hepatoma cells lines with differentiated functions in chemically defined medium. Cancer Res. **42**:3858–3863.
36. **Op De Beeck, A., C. Voisset, B. Bartosch, Y. Ciczora, L. Cocquerel, Z. Keck, S. Foung, F. L. Cosset, and J. Dubuisson.** 2004. Characterization of functional hepatitis C virus envelope glycoproteins. J. Virol. **78**:2994–3002.
37. **Pietschmann, T., V. Lohmann, A. Kaul, N. Krieger, G. Rinck, G. Rutter, D. Strand, and R. Bartenschlager.** 2002. Persistent and transient replication of full-length hepatitis C virus genomes in cell culture. J. Virol. **76**:4008–4021.
38. **Schweizer, A., J. A. M. Fransen, T. Bächi, L. Ginsel, and H.-P. Hauri.** 1988. Identification, by a monoclonal antibody, of a 53-kD protein associated with tubulo-vesicular compartment at the cis-side of the Golgi apparatus. J. Cell Biol. **107**:1643–1653.
39. **Schwer, B., S. Ren, T. Pietschmann, J. Kartenbeck, K. Kaehlcke, R. Bartenschlager, T. S. Yen, and M. Ott.** 2004. Targeting of hepatitis C virus core protein to mitochondria through a novel C-terminal localization motif. J. Virol. **78**:7958–7968.
40. **van Meer, G.** 2001. Caveolin, cholesterol, and lipid droplets? J. Cell Biol. **152**:29–34.
41. **Villanueva, R., Y. Rouillé, and J. Dubuisson.** 2005. Interactions between virus proteins and host cell membranes. Int. Rev. Cytol. **245**:171–244.
42. **Wakita, T., T. Pietschmann, T. Kato, T. Date, M. Miyamoto, Z. Zhao, K. Murthy, A. Habermann, H. G. Krausslich, M. Mizokami, R. Bartenschlager, and T. J. Liang.** 2005. Production of infectious hepatitis C virus in tissue culture from a cloned viral genome. Nat. Med. **11**:791–796.
43. **Yasui, K., T. Wakita, K. Tsukiyama-Kohara, S. I. Funahashi, M. Ichikawa, T. Kajita, D. Moradpour, J. R. Wands, and M. Kohara.** 1998. The native form and maturation process of hepatitis C virus core protein. J. Virol. **72**:6048–6055.
44. **Zhong, J., P. Gastaminza, G. Cheng, S. Kapadia, T. Kato, D. R. Burton, S. F. Wieland, S. L. Uprichard, T. Wakita, and F. V. Chisari.** 2005. Robust hepatitis C virus infection in vitro. Proc. Natl. Acad. Sci. USA **102**:9294–9299.

Production of infectious genotype 1a hepatitis C virus (Hutchinson strain) in cultured human hepatoma cells

MinKyung Yi*, Rodrigo A. Villanueva*, David L. Thomas†, Takaji Wakita‡, and Stanley M. Lemon*§

*Center for Hepatitis Research, Institute for Human Infections and Immunity, and Department of Microbiology and Immunology, University of Texas Medical Branch, Galveston, TX 77555-1019; †Department of Medicine, The Johns Hopkins University, Baltimore, MD 21231; and ‡Department of Microbiology, Tokyo Metropolitan Institute for Neuroscience, Tokyo 183-8526, Japan

Communicated by Harvey J. Alter, National Institutes of Health, Bethesda, MD, December 12, 2005 (received for review November 2, 2005)

Infections with hepatitis C virus (HCV) are marked by frequent viral persistence, chronic liver disease, and extraordinary viral genetic diversity. Although much has been learned about HCV since its discovery, progress has been slowed by a lack of permissive cell culture systems supporting its replication. Productive infections have been achieved recently with genotype 2a virus, but cirrhosis and liver cancer are typically associated with genotype 1 HCV, which is more prevalent and relatively resistant to IFN therapy. We describe production of infectious genotype 1a HCV in cells transfected with synthetic RNA derived from a prototype virus (H77-S). Viral proteins accumulated more slowly in H77-S transfected cells than in cells transfected with genotype 2a (JFH-1) RNA, but substantially more H77-S RNA was secreted into supernatant fluids. Most secreted RNA was noninfectious, banding in isopycnic gradients at a density of 1.04–1.07 gm/cm^3, but infectivity was associated with H77-S particles possessing a density of 1.13–1.14 gm/cm^3. The specific infectivity of H77-S particles (5.4×10^4 RNA copies per focus-forming unit) was significantly lower than JFH-1 virus (1.4×10^2 RNA copies per focus-forming unit). Infection with either virus was blocked by CD81 antibody. Sera from genotype 1a-infected individuals neutralized H77-S virus, but had little activity against genotype 2a virus, suggesting that these genotypes represent different serotypes. The ability of this genotype 1a virus to infect cultured cells will substantially benefit antiviral and vaccine discovery programs.

bouyant density | CD81 | cell culture | neutralizing antibody | serotype

Despite intensive research efforts, many gaps remain in our understanding of hepatitis C virus (HCV) and the mechanisms by which it causes chronic liver injury (1). To a large extent, this situation reflects the absence of tractable cell culture systems that are permissive for virus replication. Recent reports describing the efficient propagation of a genotype 2a strain of HCV, JFH-1, and a related, wholly genotype 2a chimera, FL-J6/JFH, have thus stimulated much interest (2–4). The JFH-1 virus appears to be unique among strains of HCV in terms of its ability to undergo productive infection. Many aspects of the virus–host interaction, including viral entry, assembly, and release, that were previously inaccessible to experimental manipulation, can now be studied using the JFH-1 strain and its chimeric derivatives. However, the genotype 2a JFH-1 strain is not representative of the genotype 1 strains of HCV that are principally associated with liver disease in most regions of the world (5). There is thus an important need to develop systems supporting replication of other HCV genotypes in cell culture.

Like all positive-strand RNA viruses, HCV possesses an error-prone RNA replicase. Strains of HCV show extraordinary genetic diversity, both in terms of quasi-species variation within infected individuals, as well as genetic distances between viruses belonging to different genotypes (5, 6). Pairwise differences in the nucleotide sequences of the six HCV genotypes are on the order of 31–33%. This degree of variation approximates the genetic distance between members of the classical flavivirus serogroups, such as the four dengue viruses and members of the Japanese encephalitis serogroup, that represent serologically and genetically distinct viruses (7). The extent to which critical epitopes involved in antibody (Ab)-mediated neutralization varies among different HCV genotypes is not well understood. Neutralization studies using pseudotyped retrovirus particles suggest considerable relatedness among different HCV genotypes (8), but these conclusions need to be confirmed in neutralization studies using authentic HCV. There also may be important distinctions in the capacity of different genotypes of HCV to establish long-term persistence or to cause liver disease. Cirrhosis and liver cancer are typically associated with genotype 1 viruses, which are most prevalent (5). As important, there are marked differences in the therapeutic responses of different genotypes, with genotype 1 viruses being least likely (≈45%) and genotype 2 viruses most likely (≈85%) to respond to IFN-based therapy (9). Collectively, this marked genetic heterogeneity and the corresponding clinical outcome differences underscore the importance of developing genotype 1 replication systems.

Unmodified genomic RNA derived from the genotype 2a JFH-1 strain of HCV produces infectious virus particles after transfection into Huh7 hepatoma cells (2, 3). In contrast, the genome of the prototype genotype 1a virus, H77, although capable of efficient replication in chimpanzees, replicates poorly in cell culture (10, 11). Nonetheless, we recently reported the efficient replication of H77 genomic RNA containing five adaptive mutations (referred to herein as "H77-S") in Huh7 hepatoma cells (12). These adaptive mutations are located within the NS3, NS4A, and NS5A proteins (see Fig. 1*A*). Here, we describe production of infectious HCV in cells transfected with this RNA. We compare the biophysical properties of genotype 1a and 2a particles produced in cell culture and show that these viruses can be readily distinguished serologically. Although possessing lower specific infectivity than JFH-1 virus produced in cell culture, the ability of this genotype 1a virus to infect cultured cells should substantially benefit antiviral and vaccine discovery programs.

Results

Previous studies have shown that a combination of five cell culture-adaptive mutations provide for efficient replication of the genotype 1a H77-S RNA in transfected Huh7 cells (12). To assess the ability of this highly cell-culture-adapted RNA to produce infectious virus in transfected cells, we created a related mutant, H77-S/ΔE1p7, with an in-frame deletion of sequence encoding the HCV structural proteins, E1, E2, and p7, that should eliminate virus particle formation but not impair viral RNA replication (Fig. 1*A*). Synthetic RNA transcribed from these two constructs, and an RNA replication-defective mutant containing an Ala–Ala–Gly substitution for the conserved Gly–

Conflict of interest statement: No conflicts declared.

Abbreviations: FFU, focus-forming unit; HCV, hepatitis C virus.

§To whom correspondence should be addressed at: Center for Hepatitis Research, Institute for Human Infections and Immunity, University of Texas Medical Branch, 301 University Boulevard, Galveston, TX 77555-1019. E-mail: smlemon@utmb.edu.

www.pnas.org/cgi/doi/10.1073/pnas.0510727103

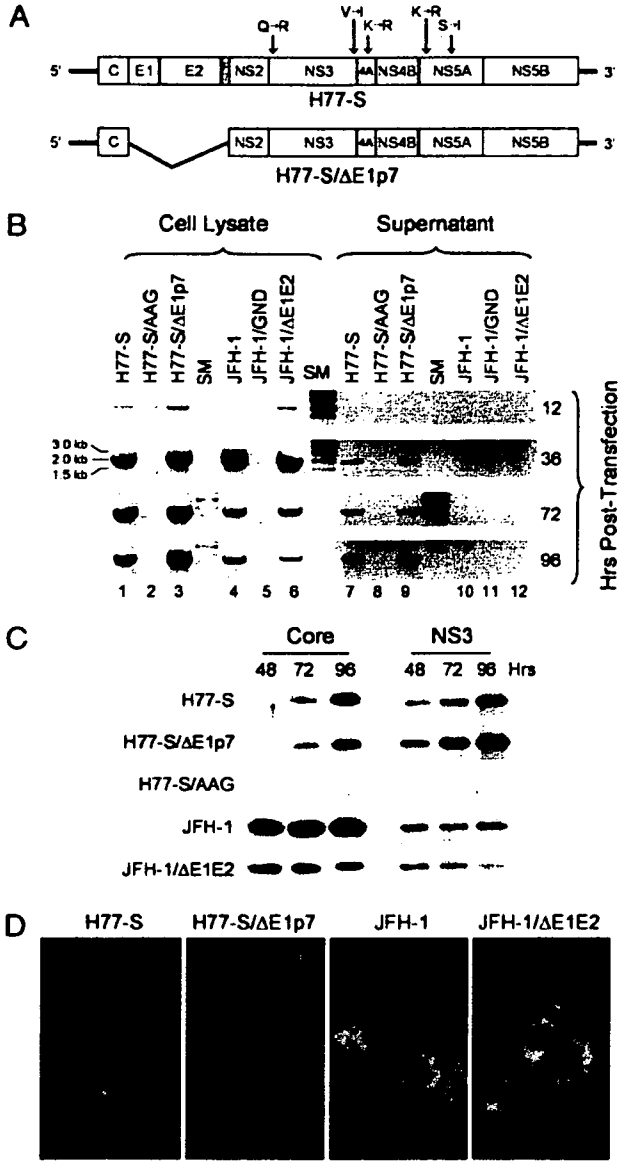

Fig. 1. Replication of H77-S and JFH-1 RNAs in transfected Huh-7.5 cells. (*A*) Organization of the H77-S genomic RNA, showing location of the five adaptive mutations and the H77-S/ΔE1p7 mutant in which sequence encoding the structural proteins was deleted. (*B*) Semiquantitative RT-PCR assays for HCV RNA in lysates (*Left*) and supernatant fluids (*Right*) of transfected Huh-7.5 cells. (*C*) Immunoblot detection of the HCV core and NS3 proteins in transfected Huh-7.5 cells. (*D*) Core antigen detected by indirect immunofluorescence 96 h after transfection of Huh-7.5 cells with the indicated RNA.

Asp–Asp motif in the NS5B polymerase active site (H77-S/AAG), were electroporated into Huh-7.5 cells. These cells are deficient in signaling virus activation of IFN-β synthesis through the intracellular retinoic acid-inducible gene I (RIG-I) pathway and are highly permissive for HCV RNA replication (13, 14). In parallel, Huh-7.5 cells were transfected with similar RNA transcripts derived from the JFH-1 virus and related mutants containing either a deletion of E1 and E2 or a Gly–Asn–Asp substitution in NS5B. Cells were monitored for replication of the transfected RNAs by a semiquantitative RT-PCR assay targeting an ≈1.9-kb segment of the NS3-coding region (see *Materials and Methods*). This assay is sensitive and specific for replication of synthetic viral RNAs after transfection.

Both the H77-S and JFH-1 RNAs replicated efficiently in Huh-7.5 cells, as did the related mutants in which the structural proteins were deleted (Fig. 1*B*, lanes 1, 3 and 4, 6). RNA synthesis was evident as early as 12 h after electroporation, with strong RT-PCR signals obtained from lysates prepared 36 h after transfection. These levels of RNA persisted in the H77-S and H77/S-ΔE1p7 transfected cells through 96 h after transfection (lanes 1 and 3), whereas the RT-PCR signal was notably decreased in JFH-1 and JFH-1/ΔE1E2-transfected cells by 72–96 h compared with that present at 36 h (lanes 4 and 6). In contrast, viral RNA was not detected in lysates of cells transfected with the NS5B mutants, indicating a failure of replication (Fig. 1*B*, lanes 2 and 5). These results were confirmed by immunoblot detection of the core and NS3 proteins in lysates of the transfected cells (Fig. 1*C*) and by immunofluorescence imaging of the core protein (Fig. 1*D*).

Several interesting differences were apparent in the expression of H77-S and JFH-1 proteins. Despite high abundance of viral RNA in H77-S transfected cells (Fig. 1*B*), JFH-1 transfected cells contained substantially more core protein, particularly at early time points (Fig. 1*C*). Core accumulated slowly in H77-S transfected cells, whereas its abundance was maximal at the earliest time point, 48 h, in JFH-1 transfected cells. Immunofluorescence staining was also substantially more intense for core antigen in the JFH-1 transfected cells (Fig. 1*D*). NS3 abundance also increased with time in H77-S transfected cells, whereas maximal levels were present at 48 h in JFH-1 transfected cells (Fig. 1*C*). The less intense NS3 signal in JFH-1 immunoblots likely reflects antigenic differences between JFH-1 and H77-S, as the NS3 Ab was raised to genotype 1a protein. In contrast, the anti-core monoclonal Ab (mAb) we used recognizes an epitope located between residues 21–40 of the protein, which is conserved in both viruses. These results suggest that JFH-1 RNA produces more core protein than H77-S RNA or that the JFH-1 core protein has greater stability than the H77-S protein in Huh-7.5 cells. However, a smaller proportion of cells expressed detectable core antigen in the JFH-1 transfected cultures 96 h after transfection (Fig. 1*D*). This difference suggests that JFH-1 RNA replication may be associated with greater cell death than H77-S.

Because Huh7 cells transfected with the JFH-1 RNA are known to release infectious virus particles (2, 3), we compared the secretion of viral RNA from these cells into the supernatant culture fluids. Substantially more viral RNA was released into supernatant fluids from H77-S transfected cells than from JFH-1 transfected cells (Fig. 1*B*, compare lanes 7 and 10), with the abundance of H77-S RNA released increasing between 36 and 96 h. In contrast, JFH-1 RNA release was minimal and detected only at 36 h after transfection in this assay. However, the release of either of these RNAs into the supernatant fluids was not dependent on expression of the envelope proteins (lanes 9 and 12), indicating that the presence of viral RNA in the culture media is not indicative of viral particle assembly.

Clarified supernatant culture fluids collected 24–96 h after transfection were tested for the presence of infectious virus by inoculation onto naïve Huh-7.5 cells, followed by fixation and staining for the presence of core antigen 96 h later. Core was present in numerous cells inoculated with the JFH-1 supernatant fluids (Fig. 2*A Right*), consistent with infection with JFH-1 virus (2, 3). Importantly, we also observed core antigen in a smaller number of cells inoculated with the H77-S supernatant fluids (Fig. 2. *Left*). As described previously for the JFH-1 virus (2), H77-S infected cells were grouped in small clusters. These clusters appear to result from division of a single infected cell during the 96-h incubation period or possibly by cell-to-cell spread of virus. Thus, in subsequent experiments, we measured virus infectivity in terms of "focus-forming units" (FFU). Im-

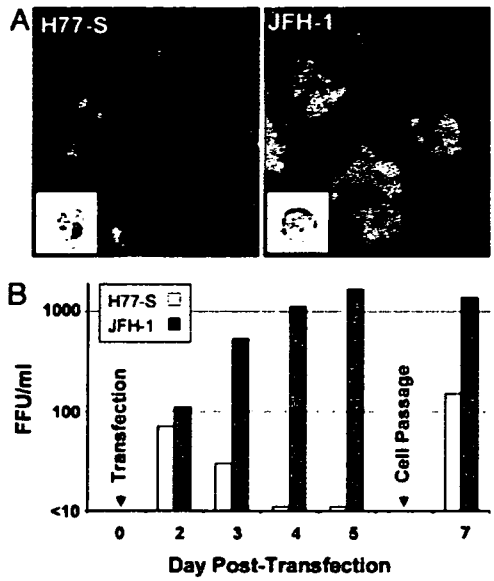

Fig. 2. Infection of Huh-7.5 cells with H77-S and JFH-1 virus released into supernatant fluids of transfected Huh-7.5 cells. (*A*) HCV core antigen expression in cells infected with H77-S (*Left*) or JFH-1 (*Right*) virus. *Left Inset* shows a particle with immunogold labeling indicating recognition by the AP33 mAb to E2. (Bar: 50 nm.) *Right Inset* shows a typical JFH-1 particle for comparison. (See also Fig. 5.) (*B*) Time course of infectious H77-S (open bars) and JFH-1 (filled bars) virus released into supernatant fluids of RNA-transfected Huh-7.5 cells. H77-S release was greatest 24–48 h after transfection or passage of cells.

portantly, the intensity of antigen staining in these cells mirrored that in the transfected Huh-7.5 cells, with less intense staining of core antigen in H77-S infected cells. Supernatant fluids remained infectious after passage through a 0.2-μm filter, consistent with cell-free virus.

Interestingly, the release of infectious virus from H77-S transfected cells was not continuous, but was greatest 24–48 h after transfection and reduced subsequently (Fig. 2*B*). Trypsin treatment of the cell monolayer, followed by a 1:3 split and reseeding of the cells at a lower density, resulted in a reproducible burst of virus production. These results are consistent with previous observations indicating that HCV RNA replication is tightly coupled to host cell proliferation and that viral RNA synthesis is enhanced during the S phase of the cell cycle (15, 16). In contrast, the release of JFH-1 virus was continuous and increased with time (Fig. 2*B*).

Electron microscopic examination of supernatant fluids from both H77-S- and JFH-1-transfected cultures revealed the presence of occasional virus-like particles measuring 44–64 nm in diameter (Fig. 2*A Insets*; see also Fig. 5, which is published as supporting information on the PNAS web site). Some particles in the H77-S infectious material bound gold-labeled mAbs to the E2 glycoprotein of HCV (Fig. 2*A Left Inset*). Importantly, neither viral antigen expression in inoculated cells nor virus-like particles were observed with supernatant fluids taken from cells transfected with the H77-S/ΔE1p7 mutant, despite equivalently robust replication of that RNA in transfected cells (Fig. 1*B*, lanes 3 and 9). Together, these results provide strong evidence for the production of cell culture-infectious H77-S virus in transfected Huh-7.5 cells. However, the lower number of antigen-positive cells obtained with inoculation of the H77-S harvest compared with the JFH-1 harvest suggests that the production of infectious virus is 10- to 100-fold less efficient with H77-S.

To compare the physical properties of infectious H77-S and JFH-1 particles, aliquots of concentrated posttransfection supernatant fluids were passed through a 0.2-μm filter and then layered onto a preformed 10–40% iodixanol gradient, which was centrifuged to equilibrium. Fractions collected from this isopycnic gradient were tested for viral RNA by the semiquantitative RT-PCR assay described above (Fig. 3*A*). Much of the H77-S RNA was present in fractions 2 to 3, near the top of the gradient, but a major fraction of the RNA banded discreetly at a higher density (≈1.13–1.14 g/cm^3) in fractions 5 to 6. Importantly, this second RNA peak was absent in gradients loaded with concentrated supernatant fluids from cells transfected with the H77-S/ΔE1p7 mutant (Fig. 3*A*). Although a small amount of JFH-1

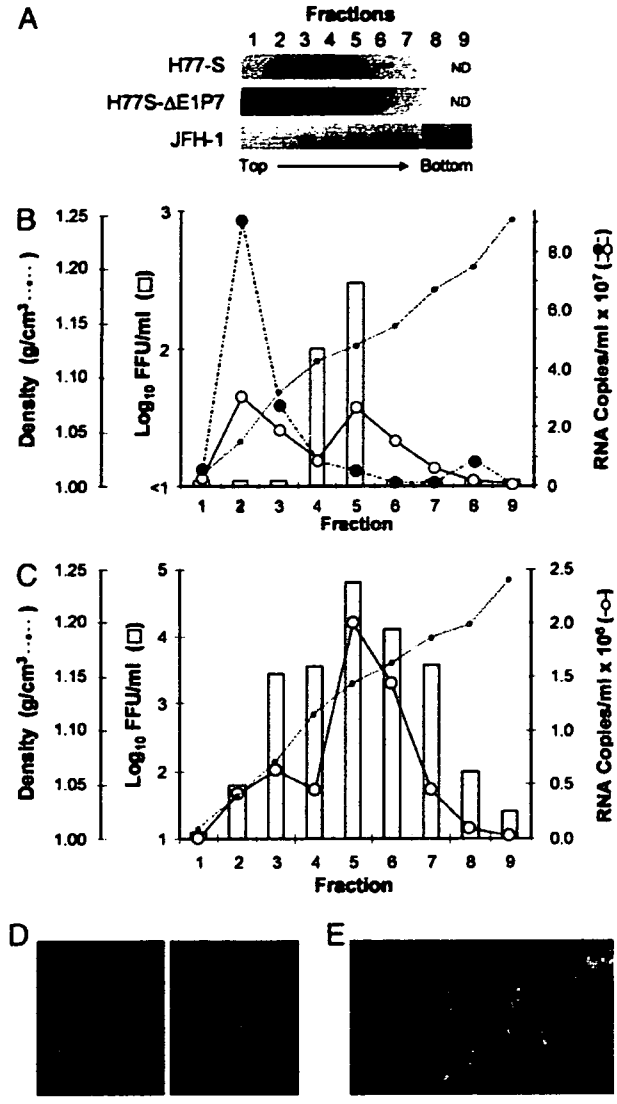

Fig. 3. Equilibrium ultracentrifugation of H77-S and JFH-1 particles in isopycnic iodixanol gradients. (*A*) Semiquantitative RT-PCR detection of HCV RNA in fractions of gradients loaded with concentrated, filtered (0.2 μm) supernatant fluids from cells transfected with the indicated RNAs. (*B*) Results of infectivity assays (bars) and quantitative TaqMan RT-PCR assays in fractions from gradients loaded with concentrated supernatant fluids from cells transfected with H77-S (solid line with open circles) or H77-S/ΔE1p7 (dashed line with filled circles) RNA. H77-S/ΔE1p7 supernatant fluids contained no infectious virus. (*C*) Results of similar assays using fractions from gradients loaded with concentrated JFH-1 supernatant fluids. (*D* and *E*) HCV core antigen detected by indirect immunofluorescence in cells inoculated with fraction 5 of gradients loaded with H77-S (*D*) or JFH-1 (*E*) material (lower magnification).